Struct Bond
DOI: 10.1007/430_2016_8

Oxo Clusters of 5*f* Elements

Sarah Hickam and Peter C. Burns

Abstract The chemistry of the 5*f* elements has been studied for decades, primarily driven by nuclear security and the nuclear-fuel cycle. A young subset of this field, the synthesis of actinide clusters, is rapidly developing and providing new insight into actinide chemistry and environmental behavior, with possible applications for the nanoscale control of these elements. The electronic character and oxidation states of the actinides strongly influence the types and diversity of structures that may be achieved. Hexavalent actinide clusters in particular have structural variety paralleling that of transition metal polyoxometalates. This is exemplified by uranyl peroxide cage clusters, which have more structural topologies than any other cluster-type examined here. This text provides an update on this still-emerging field, building on previous review articles, with a focus on oxygen-coordinated actinide clusters and the commonalities and trends between them.

Keywords Actinides • Actinyl ion • Cluster synthesis • Oxo bridges • Polynuclear

Contents

S. Hickam
Department of Civil and Environmental Engineering and Earth Sciences, University of Notre Dame, Notre Dame, IN 46556, USA

P.C. Burns (✉)
Department of Civil and Environmental Engineering and Earth Sciences, University of Notre Dame, Notre Dame, IN 46556, USA

Department of Chemistry and Biochemistry, University of Notre Dame, Notre Dame, IN 46556, USA
e-mail: pburns@nd.edu

1 Introduction

The actinide elements are a transition series generated by filling of the 5*f* orbitals. The 5*f* and 6*d* orbitals are both capable of contributing to bonding for the actinides [1], and the behavior of the 5*f* orbitals greatly influences the properties of these elements, yielding a diverse chemistry. The elements thorium through plutonium have characteristics in common with d-block elements, including covalent bonding and multiple oxidation states [1, 2]. Actinium and the actinide elements heavier than plutonium have properties that commonly link them to the lanthanide series, such as ionic character and the prevalence of the trivalent oxidation state [1]. Diverging characteristics are observed for californium and heavier elements, including that they more readily achieve the divalent oxidation state [3, 4] and californium has displayed covalent bonding [3, 5].

Actinides are radioactive heavy metals that are the fuels for nuclear reactors and atomic weapons. More than 400 nuclear plants in the world produce about 13% of all electricity, and more than 70 new plants are under construction. Actinides fuel reactors used for medical isotope production, as well as many industrial applications. They are also major constituents of irradiated nuclear fuel and various types of radioactive waste, are environmental contaminants in uranium mine and mill tailings [6], and are widespread contaminants at sites used for nuclear weapon production and testing [7, 8].

Owing at least in part to their radioactivity and strategic importance, studies of actinides have generally lagged behind those of other areas of the periodic table. Synthesis and characterization of actinide oxo clusters also lagged behind corresponding studies of the transition metals, but it is an area of substantial growth over the past decade. Such polynuclear species are of considerable interest because they can impact transport and migration behavior of actinides in the environment, related to hydrolysis and condensation [9], especially for Pu(IV) and Th(IV).

Actinide clusters, such as uranyl peroxides, have several potential applications in the nuclear-fuel cycle [10]. Furthermore, actinide oxo clusters allow for a degree of control at the nanoscale, and the probing of size-property relations.

Actinide (An) clusters have been isolated for An(IV), An(V), and An(VI) and usually exhibit characteristics that are oxidation-state specific, such as the details of the termination of the cluster structure. An(IV)-bearing clusters are typically terminated by organic ligands, but many An(VI) clusters are terminated by O atoms that are strongly bound to An(VI) cations, as part of actinyl ions (see below). Although covalent interactions between An(IV) and ligands have been observed [1], O atoms are generally not terminal ligands in An(IV) clusters, owing to their tendency to bridge to other metals, which favors extended solids. When specific ligands, usually organic, are used to passivate the surface of an An (IV) oxo cluster, clusters can be isolated. Some of the An(IV) oxo clusters have the well-known fluorite-type structure, where the An(IV) cation is coordinated to eight O atoms and each O atom is coordinated to four An(IV) cations [11].

Thorium and plutonium oxo clusters are only known to occur with tetravalent cations. Thorium is stable only in the tetravalent oxidation state in aqueous solution [2], and although plutonium occurs in multiple oxidation states in solution, only Pu (IV) clusters have been obtained, although Pu(VI) has been incorporated into a polyoxometalate sandwich complex [12]. Uranium oxo clusters have been isolated that contain U(IV), U(V), or U(VI), and in some cases combinations of U(IV) and U (V). U(V) is unstable toward disproportionation to U(IV) and U(VI) in most aqueous solutions [2].

Actinyl ions dominate the chemistry of An(V) and An(VI). In the actinyl ion, two oxygen atoms are multiply bonded to the actinide in a *trans* configuration, giving a linear $(AnO_2)^{+1,+2}$ species. The most studied actinyl ion is $(UO_2)^{2+}$, in which $5f_\sigma$-$6p_\sigma$ hybridization and $6d_\pi$ overlap with O $2p$ orbitals create a covalent metal–oxygen bond with a linear geometry [13, 14]. The average U(VI)-O_{yl} bond length is ~1.78 Å and bonding requirements of the uranyl O atoms are largely satisfied by bonds with U(VI) alone [15]. Thus, the *–yl* O atoms tend not to form strong bonding interactions with other atoms; instead, they are the terminal ligands of many U(VI) clusters, where they only participate in weaker hydrogen bonds or bonds to low-valence cations in most cases.

The preference of *–yl* O atoms to adopt a *trans* arrangement in actinyl structures has been attributed to an inverse *trans* influence (ITI) [16]. For transition metals, a strongly bound ligand weakens the bond *trans* to it, which is known as the *trans* influence, but the opposite occurs for actinide structures. The *trans* and inverse *trans* influences have been studied for MZY_5^{n-} complexes, where M is a transition metal or actinide, Z is the strongly bound oxo or nitrido group, and Y denotes a halide. The M-Y_{trans} bond is longer than M-Y_{cis} bonds for transition metals, whereas the M-Y_{trans} bond is shorter than the M-Y_{cis} bonds in actinide structures [14]. Computational studies have given insight into these observations. The polarization of the 6*p* orbitals due to the metal-oxo bond results in good parity and mixing of the 6*p* the 5*f* orbitals and quadrupolar polarization of the metal core

electrons [17, 18], and this contributes significantly to the ITI [17]. Several studies have demonstrated that the ITI is also influenced by the 5*f* orbitals [19, 20], as the ITI increases with the lowering of 5*f* orbital energy, and La Pierre et al. [17] showed that the decreased energy of 5*f* orbitals results in better parity with O 2*p* orbitals relative to N 2*p* orbitals.

Ligand attachment and polymerization occur in the equatorial plane of bipyramids about the uranyl ion, where it is coordinated to four, five, or six ligands, resulting in square, pentagonal, and hexagonal bipyramids, respectively. Typically, these units polymerize to form one- and two-dimensional structures, but in recent years many clusters have resulted from linkages of these polyhedra. For hexagonal bipyramids, the average bond length from the U(VI) cation to an equatorial O atom is significantly longer and more variable than the U-O_{yl} bond, with an average length of about 2.36–2.46 Å [21]. Sheet structures of U(VI) often contain polyhedra that share several or all equatorial edges [21] as the bonding requirements of equatorial O atoms are not entirely met by bonding to only two U(VI) cations.

Np(VI) coordination environments are very similar to U(VI), although the average Np(VI)-O_{yl} bond in inorganic structures published prior to 2008 is slightly shorter at about 1.74 Å [22]. The Np(V) neptunyl ion also displays similar coordinations; however, the difference in valence leads to significant structural differences. At 1.84 Å, the Np(V)-O_{yl} bond length is slightly longer than Np(VI)-O_{yl} and U-O_{yl} bonds, and the Np(V)-O bonds within the neptunyl ion are noticeably weaker than those in Np(VI) or U(VI) actinyl ions [22]. Often, $(NpO_2)^+$ ions are linked through the so-called cation–cation interactions (CCIs), where one *–yl* oxygen is also the equatorial oxygen atom coordinated to a neighboring actinyl ion. CCIs are pervasive in Np(V) structures – approximately 50% contain them, often as part of a framework structure [22, 23].

The first actinyl polyoxometalate cluster was reported in 2001 and contains six U(V) ions [24]. The field has experienced phenomenal growth in the last decade, starting in 2005 with the emergence of uranyl peroxide cage clusters that have been compared to the transition metal polyoxometalates [25, 26]. Highlights such as these will be discussed in this text, proceeding from tetravalent to hexavalent oxidation states. The focus here is oxo clusters published subsequent to a review by Qiu and Burns [11], with selected references to earlier structures that demonstrate a significant contribution to actinide cluster chemistry.

2 Tetravalent Actinide Clusters

Clusters with four An(IV) cations have been reported [27–29] and are examined in an earlier review [11]. The emphasis here is on clusters containing six or more An (IV) cations and, more specifically, the clusters reported since the review by Qiu and Burns [11] and those with unique terminal ligands (i.e., ligands that are not organic).

2.1 Clusters with Six An(IV) Cations

Hexanuclear clusters dominate tetravalent actinide clusters [30–39], and some have argued that these structures could be fundamental units in hydrolysis and condensation reactions of An(IV) [33]. A series of An(IV) clusters has been described that generally have the same $An_6(O,OH)_8$ composition and often have a total core composition of $[An_6(OH)_4O_4(H_2O)_6]^{12+}$, including the previously reviewed clusters containing Th(IV), [31, 33, 35], Np(IV) [34], and U(IV) [35, 38, 39], although the structure of the Np(IV) cluster was assumed on the basis of UV-vis and X-ray absorption studies of solutions [40]. Four Th(IV) and eight similar U(IV) $An_6(O,OH)_8$ clusters were reviewed previously. A fifth Th(IV) hexanuclear cluster with a $Th_6(O,OH)_8$ core has since been reported [37].

Carboxylate ligands are often used in the synthesis of hexanuclear An(IV) clusters and are incorporated as bridging and terminal ligands. A typical structure is represented in Fig. 1 and contains An(IV) cations coordinated by four bridging μ_3-O or μ_3-OH anions to form an $[An_6\{\mu_3\text{-}O,OH)_8\}]$ core. The An(IV) cations are additionally coordinated to four O atoms from a bridging ligand and an O atom from a water molecule. In the most recently reported cluster, the bridging ligand was formate [37]. Other ligands have included acetate and chloroacetate, which have been incorporated in the clusters of Knope et al. [33]. An_6O_8 structures have been obtained without carboxylate ligands, such as those by Berthet et al. [38], which were synthesized by reacting uranocene with uranyl(VI) salts, activating the strong actinyl O bonds and reducing uranium to form structures with $U_6(\mu_3\text{-}O)_8$ cores in conformations that are analogous to those described above.

The series of $An_6(O,OH)_8$ clusters has been expanded with the first Pu(IV) compound, $Li_6[Pu_6(OH)_4O_4(H_2O)_6(HGly)_{12}]Cl_{18} \cdot 10.5H_2O$ (Fig. 1) [40]. The crystals were synthesized by complexation of Pu(IV) with glycine ligands. The

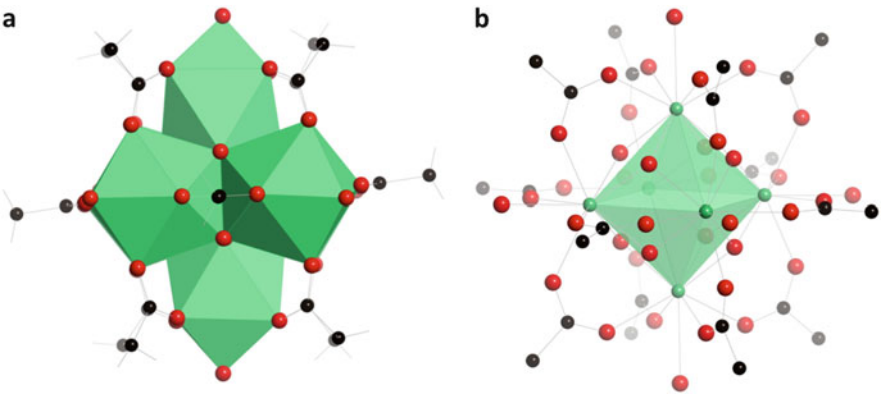

Fig. 1 (**a**) Polyhedral representation of Pu_6O_8; (**b**) the geometric arrangement of Pu atoms indicated is by a *green octahedron*. Pu is *green*, O is *red*, and carbon is *black*.

core, with composition $[Pu_6O_4(OH)_4]^{12+}$, contains Pu(IV) coordinated by nine O atoms: four are from μ_3-O/OH groups of the core, whereas the outer edges are bound to one water group and four O atoms from the glycine ligands. Cl ions balance the net +12 charge of the cluster as well as the positive charges from Li cations associated with the structure.

The $An_6(O,OH)_8$ clusters display similarities to Zr(IV) [41], Ce(IV) [42], and Bi (III) [43] clusters. For example, a Zr(IV) cluster contains atoms that are arranged at the vertices of an octahedron, are linked by μ_3-OH groups, and are bridged by glycine ligands, like many of the hexanuclear An(IV) clusters. Furthermore, a similar series of Th(IV), U(IV), Np(IV), and Pu(IV) clusters has been described that contains bridging disphosphonate ligands [30, 44]. The $An_6(O,OH)_8$ cores have also been incorporated as building units in other structures, such as U(IV) hexanuclear clusters that are identifiable in MOF-type structures [45] and Th(IV) clusters that have been linked into 3D structures through SeO_4 tetrahedra [46]. The prevalence of the An_6O_8 structural unit and variety of synthetic routes indeed seems to indicate a fundamental importance of these structures in the hydrolysis and condensation chemistry of tetravalent actinides.

2.2 Clusters with 10 or More An(IV) Ions

Two decanuclear An(IV) clusters have been reported that have $U_{10}O_{14}$ core compositions and that are terminated by organic ligands [47]. Structurally, the cores of both clusters are made up of two U_6O_8 cages that share two U(IV) cations and two O anions. With a distinct topology, the largest and only decanuclear Th (IV) compound to date, $[Th_{10}(\mu\text{-}F_{16})(\mu_3\text{-}O_4)(\mu_4\text{-}O_4)(NH_3)_{32}](NO_3)_8 \cdot 19.6\ NH_3$, was recently reported by Woidy and Kraus [48]. The core of the cluster is $[Th_{10}O_4]^{32+}$ with a topology consisting of four corner-sharing tetrahedra with Th(IV) cations at the vertices. The four μ_4-O atoms bridge Th(IV) cations in the core, which are further connected on the exterior by μ_3-O atoms. The Th(IV) cations are in three different coordination environments: four are 10-coordinate in a $[ThO_4F_3(NH_3)_3]^{7-}$ unit, and two other Th(IV) cations are coordinated to eight atoms in a $[ThO_4F_2(NH_3)_2]^{6-}$ unit. The remaining four Th(IV) cations are nine-coordinate as $[ThOF_4(NH_3)_4]^{2-}$.

While most An(IV) oxo clusters are truncated by organic ligands, four related Th(IV) octanuclear clusters and a large Pu(IV) cluster are truncated in a different fashion. In the Th(IV) structures, all of which feature a $[Th_8O_4(OH)_8]^{16+}$ core, Th(IV) cations are coordinated to nine O atoms from μ_3-O or μ_2-OH groups, water molecules, and monodentate selenate anions (Fig. 2) [9]. Selenate tetrahedra are the terminal ligands in these structures, and their additional roles include occupying "voids" in the core structures and linking multiple metal centers. The authors noted that $[Th_8(\mu_3\text{-}O)_4(\mu_2\text{-}OH)_8(SeO_4)_2]^{12+}$ and a dodecanuclear U(IV/V) cluster, $[U_{12}(\mu_3\text{-}OH)_8(\mu_3\text{-}O)_{12}]^{16+}$ [49], have structural units that are remarkably similar,

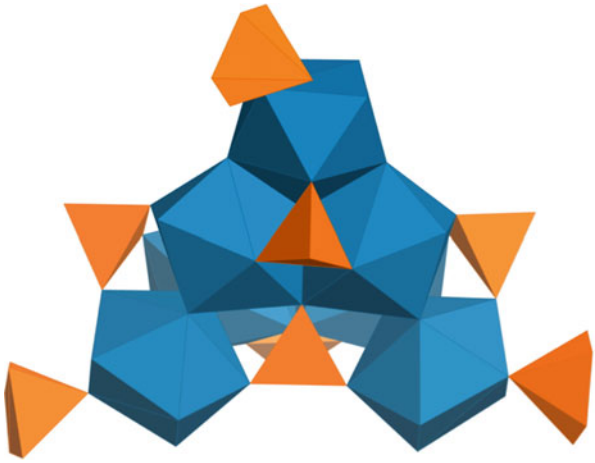

Fig. 2 The cluster terminated by selenate tetrahedra. The polyhedra are *blue* and selenate tetrahedra are *orange*

and the limited redox chemistry of Th or the influence of selenate ligands may prevent the formation of a larger Th complex.

Hydrolyzed Pu(IV) forms multinuclear metal oligomers that are of interest in Pu colloid chemistry. Crystals of $[Pu_{38}O_{56}]^{40+}$, the first oxo Pu cluster, were obtained by two different methods: (1) acidifying an alkaline peroxide solution and passing it through an anion-exchange column followed by a combination of heating and treatment with HCl and LiCl [50] and (2) recrystallizing $Li_{12}[Pu_{38}O_{56}Cl_{54}(H_2O)_8](H_2O)_x$ that was made by boiling a solution of Pu(IV) and HCl, adding LiOH, and allowing the solution to evaporate [51]. The first method produced crystals with composition $Li_{14}(H_2O)_n[Pu_{38}O_{56}Cl_{54}(H_2O)_8]$, and those from the second contain 42 Cl anions and 20 structural H_2O molecules, for a total composition of $Li_2[Pu_{38}O_{56}Cl_{42}(H_2O)_{20}] \cdot 15H_2O$. The clusters have a distorted *Fm3m* fluorite-type structure yielding a pseudocubic shape. In the first structure, H_2O groups truncate the corners and each of the six faces is terminated by Cl ions, 54 in total. The center of the cluster contains six Pu(IV) cations that are coordinated by eight shared O atoms. An additional eight Pu(IV) cations are arranged around the corners of the core, coordinated by seven O atoms and one H_2O group. The faces of the cluster contain 24 Pu(IV) cations coordinated to four O atoms and four Cl anions. In the second structure, water molecules replace 12 Cl anions.

Pu environmental transport and sorption has been extensively studied by Powell et al., who have observed Pu complexation with organic compounds in solution and nanocolloid formation on mineral surfaces [52–55]. Aqueous Pu(IV) interacts strongly with a goethite surface and forms a Pu_4O_7 nanocolloid with a distorted fluorite-type structure, as determined by HRTEM and electron diffraction [56].

Controlling the rate of hydrolysis of uranium has led to the isolation of U(IV) structures containing 10, 12, and 16 U(IV) cations [47, 49]. Utilizing this approach has more recently yielded the largest U(IV) cluster synthesized to date, $U_{38}O_{56}Cl_{18}(THF)_8(bz)_{24} \cdot 8THF$ (Fig. 3), which notably has the same nuclearity as $[Pu_{38}O_{56}]^{40+}$ [57]. The structure is related to the $Pu(IV)_{38}$ structure with a

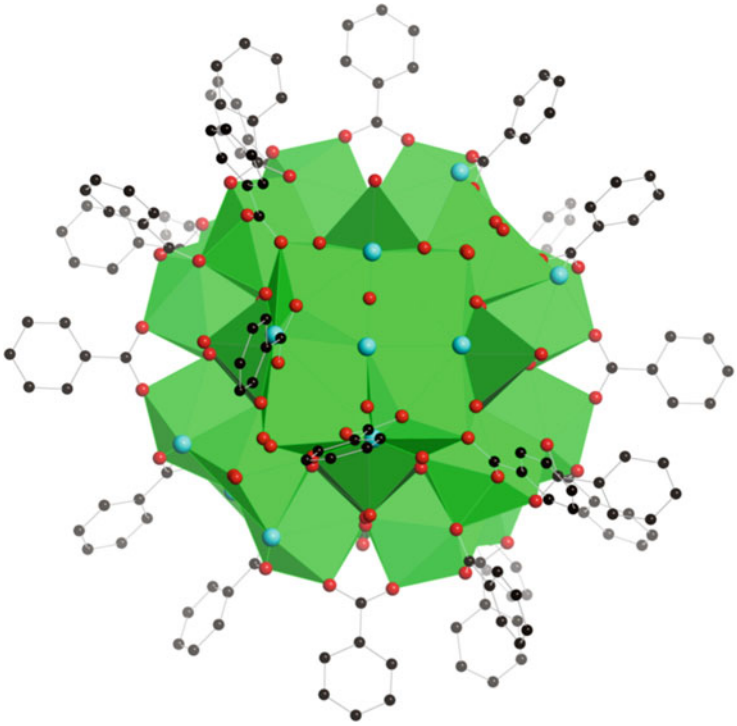

Fig. 3 Polyhedral representation of the $U(IV)_{38}$ cluster. Core U polyhedra are *dark green,* faces are *green*, Cl is *teal,* and O is *red*. Each core uranium is coordinated by a disordered benzoate molecule that is shown

fluorite-type core composed of 14 U(IV) cations in UO_8 polyhedra with cubic coordination geometry. The polyhedra are linked through edge-sharing via μ_4-O atoms. The exterior of the structure consists of six faces, each containing four U atoms. Four of the faces are identical, with two U(IV) cations in $UO_4O^{bz}Cl_3$ coordination, where *bz* indicates a benzoate ligand, and two as $UO_4O^{bz}{}_2Cl_2$. The two remaining faces have uranium atoms in $UO_4O^{bz}{}_4Cl$ coordination. Unlike $[Pu_{38}O_{56}]^{40+}$, this U(IV) cluster has benzoate terminal ligands, which occur as bidentate linkers between polyhedra and distort the structure from ideal *Fm3m* symmetry.

3 Actinide(V/VI) Actinyl Clusters

We know of only one cluster that contains Np(V) cations, a tetrameric compound with composition $[\{NpO_2(salen)\}_4(\mu_8\text{-}K)_2][K(18C6)Py]_2$ (Fig. 4) [58]. CCIs are a prevalent feature of the structure, where they connect the four Np(V) cations into a cyclic core. CCIs are becoming more important features of uranium oxo-bridged

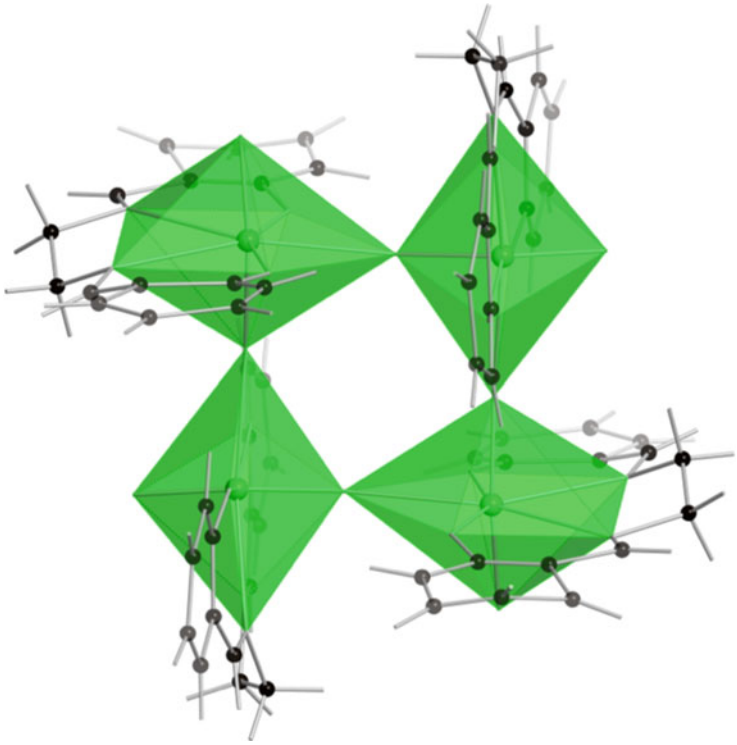

Fig. 4 Cation–cation interactions in Np(V) form a cyclic cluster

clusters as well [11]. For example, [{UO_2(salen)μ-K(18C6)}-{UO_2(salen)}$_3$ (μ_8-K)$_2$] is the first example of a uranyl cluster with CCIs between U(V) and U(VI) [59]. More discussion about CCIs in uranyl structures is provided in an earlier review [60].

Pentavalent uranium often disproportionates to U(VI) and U(IV) or oxidizes to U(VI) in solution, and as a result, the literature contains relatively few structures with U(V). One example is the largest U(V) cluster reported to date, [Cp*$_4$(bpy)$_2$] [U_6O_{13}], Cp* = 1,2,4-^{t}Bu$_3$C$_5$H$_2$, bpy = bipyridine. The core, U_6O_{13}, is analogous to the Lindqvist-type structures of molybdenum and tungsten polyoxometalates [24]. No additional U(V) clusters have been reported since the review in 2013 [11].

A large family of U(VI) peroxide cage clusters has been described in reviews published in 2011 and in 2013 [11, 61]. The focus here is an overview of uranyl peroxide cage clusters, with more detailed structural descriptions for some recently reported clusters and those with novel topological features. The Qiu and Burns [11] review indicated that all actinide clusters containing 18 or more actinide ions, with the sole exception of $Pu_{38}O_{56}$, were actinyl peroxide clusters [11]. This is no longer the case owing to the report of $U_{38}O_{56}$ and a new wheel-shaped cluster that contains 20 uranyl cations [62, 63]. The following sections explore these and other new developments.

The uranyl peroxide clusters are designated with the notation $U_xV_yW_z$, where *U* is the number of uranyl (or neptunyl in one case) ions within a cage. *V* and *W* designate structural components of the cage in addition to the uranyl ions, such as *Ox* for oxalate, *Pp* for pyrophosphate, *PCP* for methylenediphosphonate, and *L* for etidronic ligands. Finally, *x*, *y*, and *z* denote the number of each unit contained within a cluster as well as any relevant alphanumeric descriptors of topology, such as "R" for ring.

4 Uranyl Peroxide Cage Clusters

The first actinyl peroxide cage clusters were reported in 2005 and were U_{24}, U_{28}, U_{32}, and Np_{24} (Fig. 5) [25]. After a decade of exhaustive exploratory syntheses, about 60 uranyl peroxide clusters have been published that demonstrate a remarkably diverse family: some have fullerene topologies, including U_{60} (Fig. 5e) [64] that is topologically identical to C_{60} [65], others are incomplete cages with open bowl-shapes [66], and additional topologies include core-shell structures [67, 68] and one cluster with multiple, fused cages [69]. The smallest member of this family contains 16 uranyl polyhedra, whereas the largest has 124 [69]. These topologies

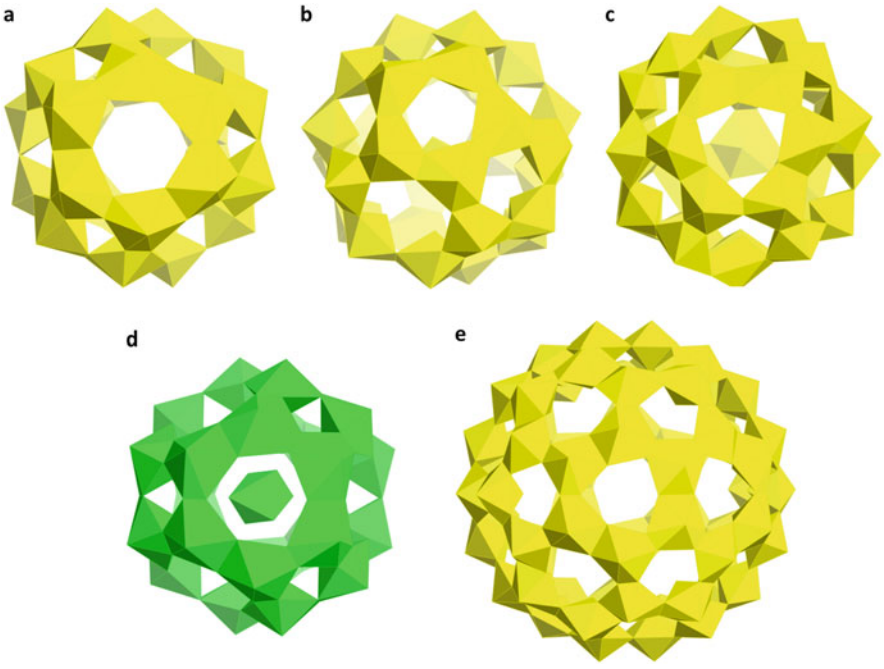

Fig. 5 The first actinyl peroxide cage clusters and those with typical topologies, including fullerene topologies. (**a**) U_{24}, (**b**) U_{28}, (**c**) U_{32}, (**d**) Np_{24}, and (**e**) U_{60}

have generally resulted by mixing uranyl nitrate and excess hydrogen peroxide, followed by the addition of other solvents and cations, and clusters have formed in solutions with pH ranges of 4–11.5 [70]. Normally, these steps are completed under ambient conditions; only U_{50} and U_{40} were crystallized after exposure to nonambient conditions by heating the solutions to 80°C in sealed Teflon-lined vials [71].

Expansion of the uranyl peroxide cage cluster family may lead to applications and new understanding, such as in the nanoscale control of materials in the nuclear-fuel cycle [10] and transport of actinides in the environment [72]. Mass-based separation of uranium peroxide cage cluster species from solutions has been achieved using ultrafiltration [10] and mesoporous silica (SBA-15) material sequestration [73]. As much as 95% rejection of U is achieved via ultrafiltration when the uranyl ions are contained in clusters, and SBA-15 extracts uranyl peroxide cage clusters from solution with an extraction capacity of 6.77 mg g^{-1}, corresponding to 97.1% efficiency.

4.1 Actinyl Coordination and Arrangement

Uranium atoms in cage clusters are strongly bonded to *trans-yl* O atoms, forming the linear dioxo cation $(UO_2)^{2+}$ that lies approximately perpendicular to the cluster surface. The *–yl* oxygen atoms passivate both the inner and outer surfaces of the structure. Five or six additional oxygen atoms are coordinated equatorially to the U(VI) cation, yielding pentagonal and hexagonal bipyramids, although hexagonal bipyramids are far more common in uranyl peroxide clusters. In most uranyl peroxide clusters, four, five, or six uranyl hexagonal bipyramids are arranged in rings by sharing equatorial edges, yielding topological square, pentagonal, and hexagonal units in the cluster structures (Fig. 6). These units are linked by edge-sharing, such that each uranyl polyhedron shares edges with three other uranyl polyhedra. However, as new structures have continued to emerge, novel topologies have been established. For example, uranyl polyhedra have been linked into belts instead of rings (Fig. 6) [60, 74] and crown- and ring-shaped clusters such as U_{20R} and U_{24R} contain hexagonal bipyramids with both two and three shared edges [66].

4.2 Peroxide Bridges

Peroxide bridges appear to be essential in cage clusters as bridging ligands between uranyl polyhedra, where two or three of the shared edges of polyhedra are peroxo groups that are bidentate to the uranyl ions. The peroxo edges of uranyl polyhedra are ~1.45 Å long, much shorter than the ~2.8 Å length typical in the absence of peroxide, resulting in distorted hexagonal or pentagonal bipyramids. U_{20}, U_{28}, and U_{44} are rare examples of clusters that contain only triperoxide polyhedra [25, 64,

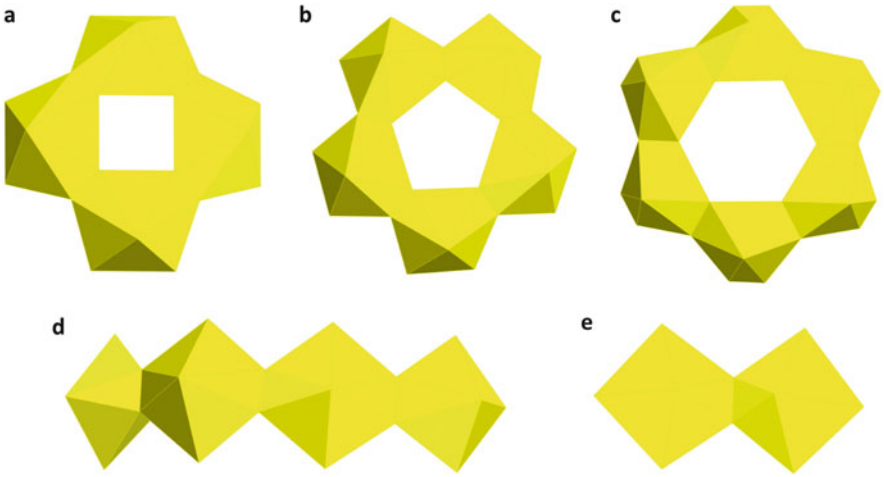

Fig. 6 Arrangements of actinyl polyhedra found in uranyl peroxide cage clusters, including (**a**) square faces, (**b**) pentagonal faces, (**c**) hexagonal faces, (**d**) belts, and (**e**) dimers

75], and polyhedra with one peroxo group have also been reported [76] but are rare. The influence of peroxide on the cage cluster topology is related to two properties: the bonding requirements of peroxide limit the number of connections between uranyl polyhedra, and the U-O_2-U bridge is highly pliable. The formal valence of peroxide is 2-, and each peroxo O atom that forms bonds to two U(VI) atoms contributes ~1 *valence unit*, satisfying the bond valence requirement [71]. Thus, connectivity in the cage clusters is limited to one, two, or three shared edges between uranyl polyhedra, and the resulting porous nature is conducive to forming a cage structure.

The characteristic curvature of the cage clusters is a result of the bent U-O_2-U dihedral angles, which range from ~130° to 155° [77]. A prevalent hypothesis has been that peroxide bridges are inherently bent and thus facilitate cage cluster formation [75]. Density function theory (DFT) studies of the U-O_2-U bridges found only a modest, 0.5 kcal mol^{-1} energy advantage of a bent dihedral angle compared to 180° in the absence of counterions [78]. Qiu et al. [79] further probed the role of hydrogen peroxide in cage cluster formation by synthesizing a variety of uranyl peroxide dimers coordinated by various organic ligands. Six of the 15 dimers had U-O_2-U dihedral angles of 180°, inconsistent with the hypothesis that the peroxide bridge is inherently bent. Nevertheless, the U-O_2-U bridge is certainly flexible and thus is an ideal ligand for the formation of cage clusters.

4.3 Roles of Alkali Ions

Counterions are essential components of uranyl peroxide cage structures that balance the large negative charges of the structural units. Although the full extent of their role in directing cluster formation is still not well understood, different

counterions are generally associated with specific rings of uranyl polyhedra [78]. K, Li, and Na are the most common counterions in the synthesis of uranyl peroxide clusters and are typically located both on the exterior of the clusters and as encapsulated species in the solid state. Unfortunately, understanding their roles is complicated by the difficulty of locating Li in X-ray structures and cation disordering in general. Two-dimensional ^{7}Li-^{7}Li magic angle spinning nuclear magnetic resonance (MAS NMR) exchange experiments indicate that Li can be highly mobile in these clusters in the solid state, exchanging between encapsulated and other lattice sites [80]. Li has only been located in the structures of Np_{24} and a LiK salt of U_{24} to date [25, 80].

DFT calculations combined with multiconfigurational methods (CASSCF/CASPT2) indicate that the U-O_2-U dihedral angle is affected by intermolecular interactions with, and the sizes of, the countercations, with a correlation between increasing angle and increasing ionic radius of the cations [77, 79]. Additionally, the U-O_2-U angle for a $[(UO_2)_2(O_2)_5]^{6-}$ cluster optimized to 180° without the addition of cations and to 145° with the addition of Na cations [77]. Counterions thus seem to favor bent U-O_2-U configurations, and may even result in different angles and therefore curvature in the resulting cages.

Cations can influence the topology of uranyl peroxide clusters by their associations with four-, five-, or six-membered rings, either by templating or by stabilizing the rings of polyhedra [78]. In general, the smaller alkali cations, Li and Na, are associated experimentally with square faces, or four-membered rings of polyhedra, while medium-size alkalis favor pentagonal faces and large alkalis occupy sites of hexagonal faces [70, 81]. DFT calculations by Miro et al. [78] support these observations. The calculations indicate that topological squares and pentagons provide bonding environments that both favor Na when it is present but, when Na is absent, Li is most suitable for square sites and K fits the topological pentagons. In the Na and Li salts of U_{24}, the encapsulated cations are located under the square face, while the larger K cations in the LiK salt are located under the hexagonal face [25, 80]. These observations are consistent with the general trends because K cations prefer the larger available sites of the cluster [80]. Due to the nature of the experiment, more specifically that the cations were exchanged after the anions were assembled, the results do not imply that K cations template six-membered rings of polyhedra. In U_{60}, for example, K occupies sites of the five-membered rings although the cluster contains both pentagonal and hexagonal faces [64]; thus, the observations from the U_{24} experiments are merely an example of the trend.

Miro et al. [78] noted that the six-membered rings of uranyl ions in uranyl peroxide cages are typically linkages between the more stable tetramers and pentamers. DFT calculations indicate that alkali cations do not have a significant stabilizing affect on hexagonal rings; nevertheless, Cs and Rb are the most suitable cations for these sites. Experimentally, less evidence exists for the influence of Cs and Rb compared to the smaller alkali cations, but two clusters, U_{24R} and U_{28}, have been published with the larger cations in the expected sites [66, 82]. Nyman et al. [82] have accomplished a more comprehensive study in which U_{28} was synthesized with combinations of K, Rb, and Cs cations. Indeed, Rb and Cs cations exclusively occupied sites of the six-membered rings of uranyl polyhedra.

4.4 Hydroxyl and Functionalized Bridging Ligands

Select shared polyhedral edges in numerous cage clusters correspond to two hydroxyl groups, forming U-$(OH)_2$-U bridges. These bridges are typically slightly bent in cage clusters, although computational studies find that the lowest energy is achieved for a U-$(OH)_2$-U dihedral angle of 180° [77]. The authors noted that a bent angle is not prohibited, and cations that bridge uranyl O atoms may encourage such bending. Many studies of uranyl peroxide cage clusters have focused on the incorporation of other ligands, including pyrophosphate, phosphite, nitrate, methylenediphosphonate, and oxalate (Fig. 7) [67, 70, 74, 83, 84]. Of these, pyrophosphate and oxalate have been extremely fruitful, because they assume "side-on," bidentate configurations with lengths that are suitable for coordination to the uranyl ion [70]. In several cases, these ligands replace hydroxyl bridges in a topologically identical cluster, such as the pyrophosphate ligands in $U_{24}Pp_{12}$, which is topologically identical to U_{24} [25, 70]. Similarly, oxalate ligands in $U_{60}Ox_{30}$ are in the place of hydroxyl bridges in U_{60} [64, 84]. $U_{30}Pp_{10}Ox_5$ contains both pyrophosphate and oxalate ligands [83]. In $U_{30}Pp_{12}P_1$, two pyrophosphate groups share all six available vertices with four different hexagonal bipyramids instead of the typical coordination of four O atoms shared with two hexagonal bipyramids [74].

Recent studies report incorporation of carboxyphosphonate [85] and (1-hydroxyethane 1,1-diphosphonic) etidronic acid [86] into uranyl peroxide cage clusters. Etidronic acid bridges uranyl ions in a fashion that is analogous to pyrophosphate and methylenediphosphonate; however, the use of this ligand,

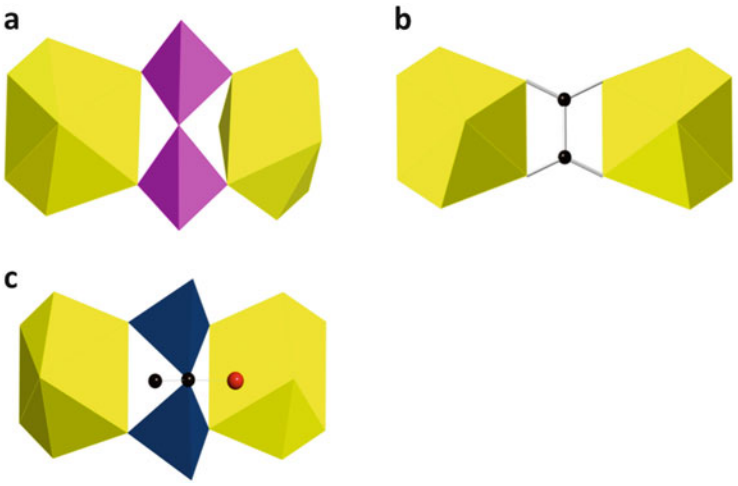

Fig. 7 Typical ligand coordination to uranyl ions is shown as (**a**) pyrophosphate, (**b**) oxalate, and (**c**) etidronic ligands

which contains larger functional groups on the bridging C atom, has yielded novel topologies discussed below.

4.5 *Novel and Complex Topologies in Uranyl Peroxide Cage Clusters*

$U_{22}PO_3$ and $U_{28}PO_3$ are the first reported chiral uranyl peroxide clusters [60]. The composition of the $U_{22}PO_3$ cage is $[(UO_2)_{22}(O_2)_{15}(HPO_3)_{20}(H_2O)_{10}]^{26-}$ (Fig. 8a, b), and the cage is charge balanced by disordered K counter cations or both K and Na cations. $U_{28}PO_3$ has composition $[(UO_2)_{28}(O_2)_{20}(HPO_3)_{24}(H_2O)_{12})]^{32-}$ (Fig. 8c, d) and has only been reported with K countercations. The syntheses of these crystals are similar to those reported for other uranyl peroxide cage clusters, except that ethylenediaminetetraacetic acid dipotassium salt and $NaNO_3$ are the sources of cations. $U_{22}PO_3$ and $U_{28}PO_3$ crystallize across the limited pH range of

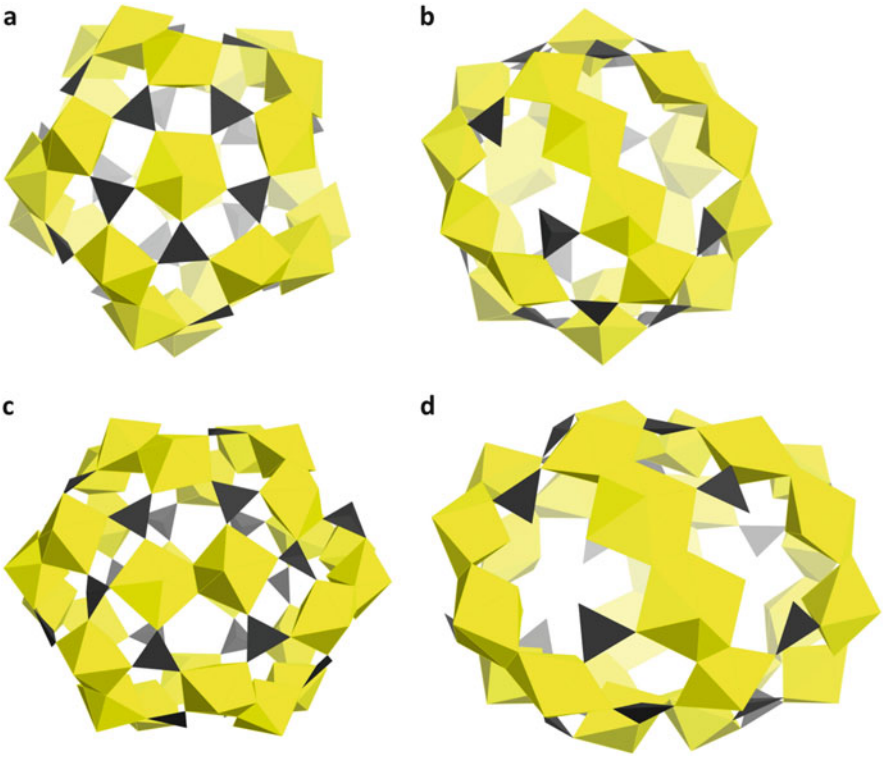

Fig. 8 Chiral uranyl peroxide cage clusters are shown containing belts of polyhedra that are linked to the poles by phosphite groups, shown in *black*. (**a**) and (**b**) are the poles and equatorial regions of $U_{22}PO_3$, respectively. (**c**) and (**d**) are the equivalent features in $U_{28}PO_3$

5.2–6.5. They are the first cage clusters to contain hexagonal bipyramids with bidentate peroxide ligands in a *trans* configuration. The *trans* configuration of peroxide polyhedra gives belts of polyhedra, rather than rings, in both clusters. The belts consist of four polyhedra arranged with two pentagonal bipyramids at the ends and two hexagonal bipyramids toward the center, which are all bridged by bidentate peroxide ligands. The pentagonal bipyramids of the belt are also coordinated to three $(HPO_3)^{2-}$ ligands, one of which links the belt to the pole and two that connect adjacent belts. $U_{22}PO_3$ contains five of these belts and has poles terminated by pentagonal bipyramids coordinated by five $(HPO_3)^{2-}$ ligands. $U_{28}PO_3$ has six belts bridged in the same manner and poles consisting of dimers in the form of two bidentate peroxo-bridged pentagonal bipyramids, which are coordinated to a total of six $(HPO_3)^{2-}$ ligands.

$U_{22}PO_3$ and $U_{28}PO_3$ crystallize as enantiomorphic pairs of right- and left-handed structures. The *trans* configuration of peroxo ligands is also found in the infinite chains in studtite, although it had not been reported in a uranyl peroxide cage cluster [87]. The two pole configurations are also novel: $U_{22}PO_3$ is the first uranyl peroxide cluster to contain pentagonal bipyramids with no peroxide ligands, and $U_{28}PO_3$ is the first to contain uranyl pentagonal bipyramids linked through peroxo bridges. Interestingly, no relationships between the Na or K cations and the belts of polyhedra were observed, and the authors suggested that these clusters might assemble by a different mechanism than those containing rings, for which the cations play a significant role.

Some of the most complex uranyl peroxide cage clusters consist of core-shell units. U1 ⊂ U28 ⊂ U40R contains a core cage of 28 triperoxide and diperoxide uranyl hexagonal bipyramids with fullerene topology that has a U atom at the center [68] (Fig. 9a). Surrounding this core, 40 uranyl polyhedra occur as pentamers that are linked, along with nitrate groups, into a bent ring-shaped shell. 40 K cations are located between and connect the two units by coordinating to –*yl* and peroxo O atoms. The authors suggested that the shell is templated by the core structure, because topological pentagons of the shell are located above pentagons of the core structure. Additionally, the assembly of the shell is delayed by 2 weeks compared to the core, as indicated by electrospray ionization mass spectrometry (ESI-MS) and small-angle X-ray scattering (SAXS) data.

$U_{120}Ox_{90}$ [67] has a core that is identical to $U_{60}Ox_{30}$ [84]. Instead of a fully connected shell structure, 12 separate five-membered rings of uranyl hexagonal bipyramids, terminated by oxalate groups coordinated to each uranyl ion, are arranged around the core (Fig. 9b). Similarly to U1 ⊂ U28 ⊂ U40R, K cations connect the core structure to the five-membered rings of the shell, and the core most likely templates the shell structure.

The largest uranyl peroxide cage cluster synthesized to date is $U_{124}P_{32}$, which has a composition $K_xLi_y[(UO_2)_{124}(O_2)_{152}(PO_4)_{16}(HPO_4)_8(H_2PO_4)_8(OH)_4(H_2O)_{24}]$ H_2O_n (Fig. 9c). Compared to previously published uranyl peroxide cage clusters, the high degree of complexity of $U_{124}P_{32}$ is unequivocal: it is composed of five cages within a single cluster. Four of the five cages are symmetrically identical, and

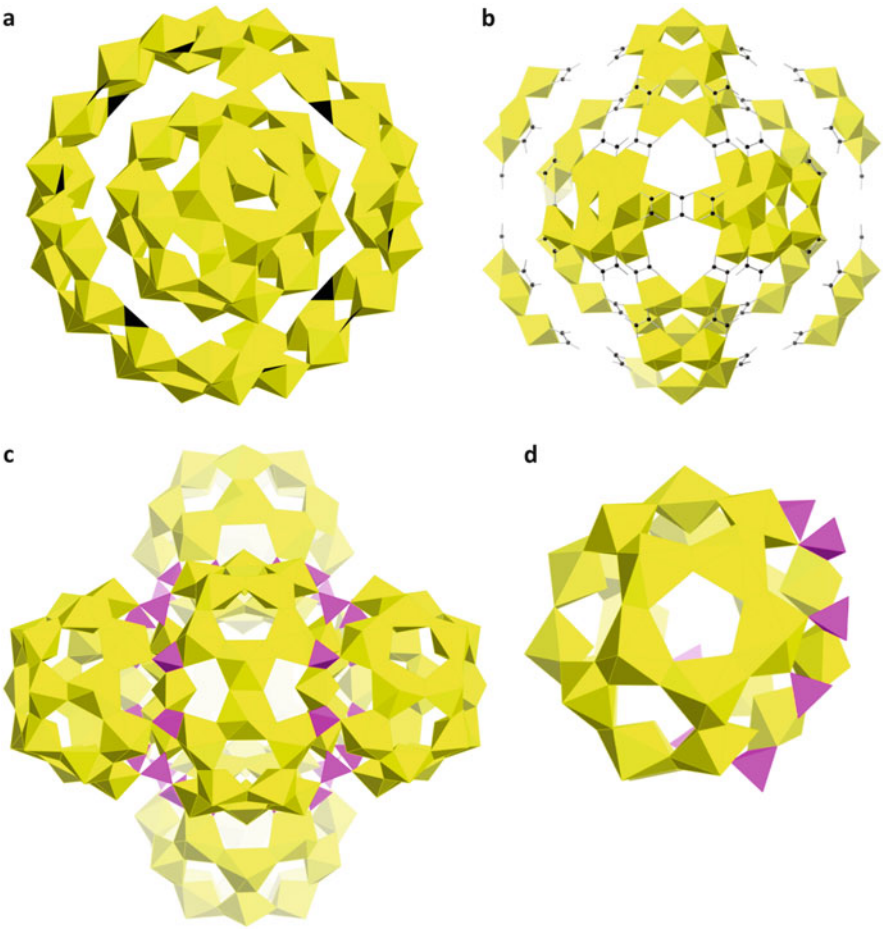

Fig. 9 Complex topologies in uranyl peroxide cage clusters including (**a** and **b**) core-shell clusters and (**c**) the multi-cage cluster containing 124 uranyl ions. One of the cages from the multi-cage structure is shown in (**d**). Nitrate groups are *black triangles,* C atoms are *black spheres*, and phosphate tetrahedra are *pink*

each contains 23 uranyl hexagonal bipyramids that are arranged into five-membered rings and one six-membered ring (Fig. 9d). One of the pentamers is connected by phosphate tetrahedra to the rest of the cage. These four cages are arranged geometrically as vertices of a tetrahedron. Two separate units of four five-membered rings of polyhedra fuse the four "vertices" together, forming a fifth cage in the center of the structure.

4.6 *Expanding the Family of Cage Clusters with Organic Ligands*

Inclusion of organic ligands has yielded uranyl peroxide-based structures, including one that contains two uranyl peroxide tetramers linked by ethylenediaminetetraacetate (EDTA) ligands [88]. Several cage clusters incorporate oxalate or methylenediphosphonate [70]. In recent years, new topologies of uranyl peroxide cage clusters have been achieved using carboxyphosphonate and etidronic ligands. Although *–yl* O atoms quite often passivate the surfaces of uranyl peroxide cage clusters, the addition of larger organic ligands into the structural units of these cage clusters provides the opportunity for organic ligands to act as terminal ligands.

Two uranyl-carboxyphosphonate cage clusters have been synthesized: $\{[K_{18}Li_4][(UO_2)_{20}(HO_2CC_6H_4PO_3)_{10}(O_2)_{20}(OH)_{10}](H_2O)_n\}^{8-}$ and $\{[K_3][(UO_2)_{24}(HO_2CC_6H_4PO_3)_8(O_2)_{24}(OH)_8]\text{-}(H_2O)_n\}^{21-}$ [85], with disordered counterions required for charge balance. $\{[K_{18}Li_4][(UO_2)_{20}(HO_2CC_6H_4PO_3)_{10}(O_2)_{20}(OH)_{10}](H_2O)_n\}^{8-}$ contains two five-membered rings of hexagonal bipyramids and a belt of uranyl polyhedra (Fig. 10a). A topological belt was earlier reported for $U_{22}PO_3$ and $U_{28}PO_3$ (see above), but it is unique in this cluster because it consists of 10 uranyl ions in a closed ring around the equatorial region. Carboxyphosphonate groups connect the belt to the two rings of uranyl polyhedra through the phosphonate moiety, whereas the carboxylate units donate oxygen atoms to uranyl polyhedra of the tetramers. The carboxylate moieties project outward in this structure and decorate the elongated exterior edges. In doing so, they act as terminal ligands for the elongated faces, while *–yl* O atoms terminate the poles.

$\{[K_3][(UO_2)_{24}(HO_2CC_6H_4PO_3)_8(O_2)_{24}(OH)_8]\text{-}(H_2O)_n\}^{21-}$ also has belts of polyhedra (Fig. 10b); however, the connectivity of the belts is different from those previously described. The belt is a ring with a circumference of eight

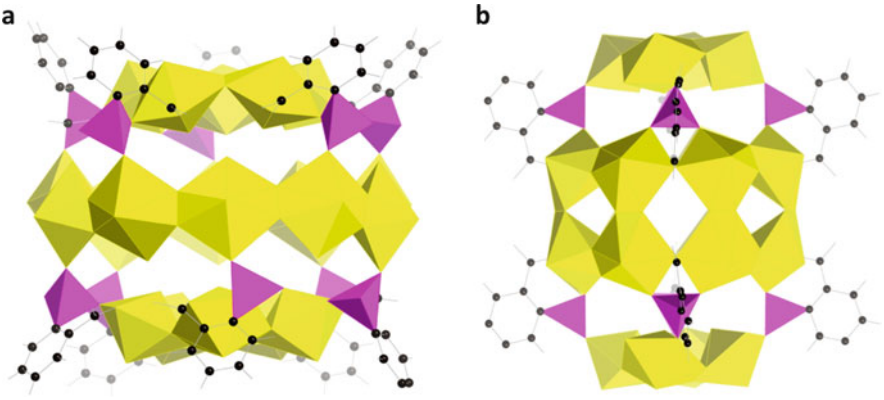

Fig. 10 The uranyl peroxide cage clusters with carboxyphosphonate ligands, (**a**) $\{[K_{18}Li_4][(UO_2)_{20}(HO_2CC_6H_4PO_3)_{10}(O_2)_{20}(OH)_{10}](H_2O)_n\}^{8-}$ and (**b**) $\{[K_3][(UO_2)_{24}(HO_2CC_6H_4PO_3)_8(O_2)_{24}(OH)_8]\text{-}(H_2O)_n\}^{21-}$. Carboxyphosphonate ligands are shown as phosphonate moieties in *pink* and carbon of the carboxyl moieties in *black*

corner-sharing polyhedra that is two polyhedra wide, formed by edge-sharing of peroxo groups. Both poles of the cluster are four-membered rings of polyhedra connected to the belt by oxygen atoms of the phosphonate groups. Instead of donating oxygen to the uranyl polyhedra of the four-membered ring, as in the previous structure, the carboxylate moieties donate oxygen atoms that connect polyhedra of the belt, linking the dimers of polyhedra to each other through corner-sharing [85].

Six cages contain (1-hydroxyethane 1,1-diphosphonic) etidronic acid ligands: $U_{24}L_{12}$, $U_{40}L_{20}$, $U_{64}L_{32}$, $U_{16}L_8$, $U_{20}L_{10}$, and $U_{16}L_8P_4$, where L indicates $[(PO_3)_2C(OH)CH_3)]^{4-}$ and P is PO_4^{3-} [86]. The use of etidronic ligands yields both known and novel topologies. Etidronic acid ligands are coordinated to a uranyl ion by two oxygen atoms and provide the linkages between rings of polyhedra in the cage structures.

$U_{16}L_8$ and $U_{20}L_{10}$ may be compared with $\{[K_{18}Li_4][(UO_2)_{20}(HO_2CC_6H_4PO_3)_{10}(O_2)_{20}(OH)_{10}](H_2O)_n\}^{8-}$ and $\{[K_3][(UO_2)_{24}(HO_2CC_6H_4PO_3)_8(O_2)_{24}(OH)_8]\text{-}(H_2O)_n\}^{21-}$ [85], because a belt of polyhedra forms a ring around the equatorial region of the cluster, whereas rings of polyhedra are at the poles (Fig. 11a, b). Two uranyl configurations define the elongated structure of $U_{16}L_8$: four-membered rings and an eight-membered belt. The belt of uranyl hexagonal bipyramids forms a ring around the equatorial region of the cluster and polyhedra are connected by edge-sharing of peroxide in a *cis* arrangement, creating a zig-zag pattern. The belt is connected to the terminating four-membered rings through the side-on etidronic ligands. Like $U_{16}L_8$, $U_{20}L_{10}$ is capped at either end by rings of uranyl polyhedra and has a belt around the center of the cluster; however, the units in $U_{20}L_{10}$ are larger, as it has two pentamers and a 10-membered belt. This cage has a fullerene topology and is isostructural to $U_{20}Py_{10}$ [70]. K cations are associated with the five-membered rings of polyhedra. Lithium hydroxide was used in the synthesis of all of the uranyl-etidronic ligand clusters and Li is assumed to be in the structures, although the cations were not identified.

$U_{24}L_{12}$, $U_{40}L_{20}$, and $U_{64}L_8$ contain four-membered rings of uranyl polyhedra formed by edge-sharing via U-O_2-U bridges in a *cis* arrangement. $U_{24}L_{12}$ is topologically identical to $U_{24}Pp_{12}$ with etidronic ligands in the place of pyrophosphate (Fig. 11c). One of the rings in $U_{24}L_{12}$ is concave outwards, whereas all rings are concave inwards in $U_{24}Pp_{12}$. Ten four-membered rings of polyhedra connected by etidronic ligands define the novel $U_{40}L_{32}$ cage (Fig. 11d). $U_{64}L_{32}$ also has a novel configuration with 16 rings (Fig. 11e, f). Na cations are located on the concave inwards side of each of the four-membered rings, with half inside and half outside the cluster.

The cluster $U_{16}L_8P_4$ has several unique features (Fig. 11g). Similar to $U_{16}L_8$, $U_{16}L_8P_4$ is terminated at two ends by four-membered rings of polyhedra; however, the central region of $U_{16}L_8P_4$ is quite different from $U_{16}L_8$ and $U_{20}L_{10}$ because it contains dimers of uranyl pentagonal bipyramids. These dimers do not contain peroxide and, instead, are bridged by the sharing of edges defined by two hydroxyl groups. The dimers are connected by $(PO_4)^{3-}$ tetrahedra. Another unique feature of $U_{16}L_8P_4$ is a tetramer occupied by K, an observation that is a departure from the

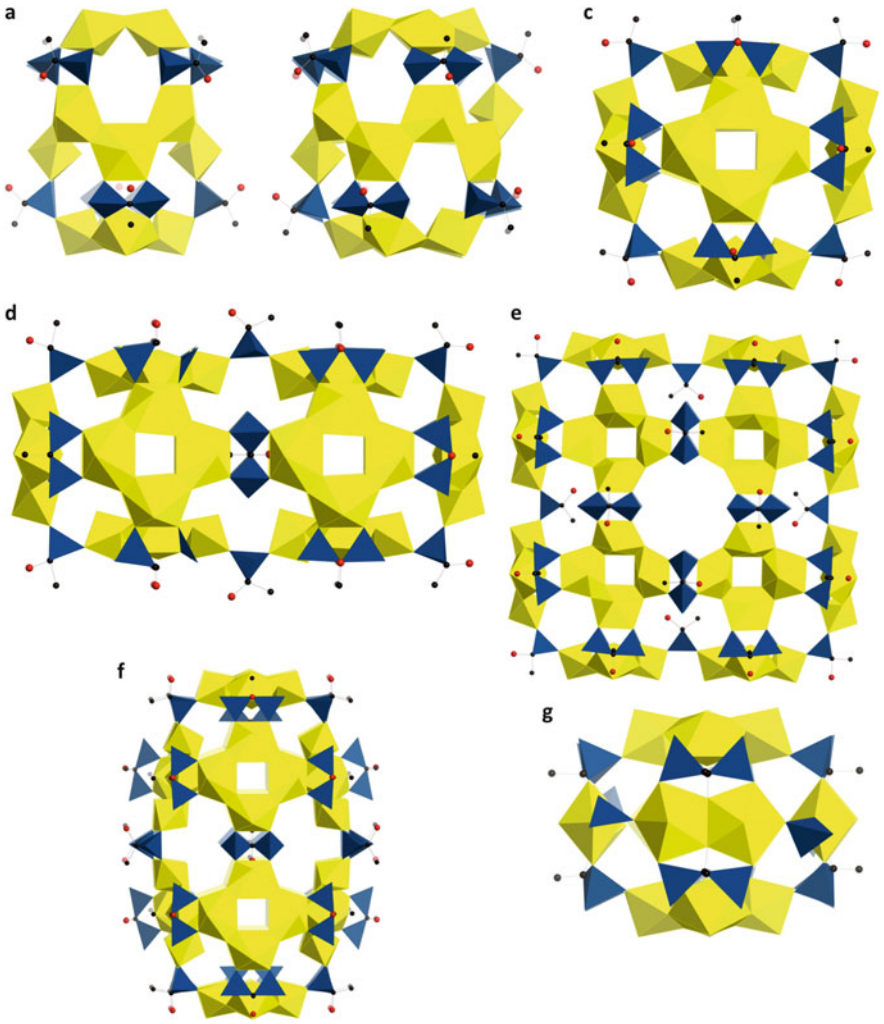

Fig. 11 The clusters (**a**) $U_{16}L_8$, (**b**) $U_{20}L_{10}$, (**c**) $U_{24}L_{12}$, (**d**) $U_{40}L_{20}$, (**e** and **f**) $U_{64}L_{32}$, and (**g**) $U_{16}L_8P_4$ that contain etidronic ligands, shown in *blue*

general trend for uranyl peroxide cage clusters. Other four-membered rings are either vacant or are occupied by Li.

4.7 Uranyl Cage Clusters Without Peroxide

The incorporation of peroxo ligands has proven to be an indispensable tool for the synthesis of large An(VI) clusters. Recently, however, several clusters were synthesized that have broadly similar structures but without peroxide ligands.

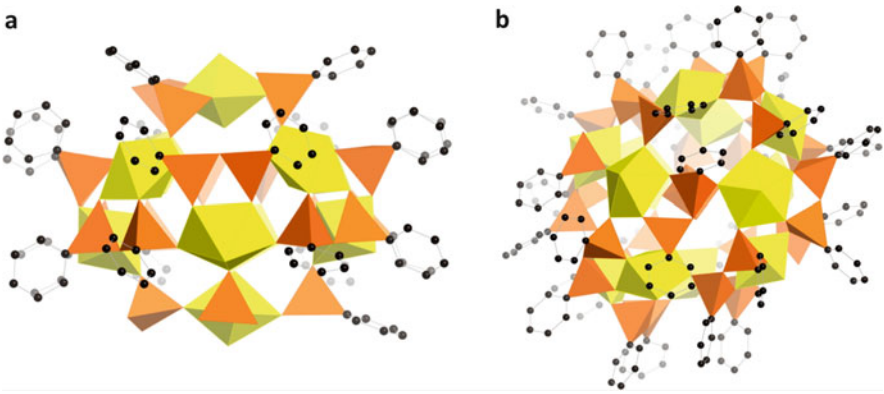

Fig. 12 Uranyl clusters containing monomers of (**a**) 10 and (**b**) 12 uranyl polyhedra connected by pyroarsonate and phenylarsonate groups, in *orange*

Adelani et al. [89] explored the use of pyroarsonate ligands in uranyl cage cluster formation with the strategy of synthesizing pyroarsenate in situ to enhance the flexibility of the ligand. From these studies, two clusters were formed: $[H_3O]_6\{(UO_2)_{10}[(C_6H_5)_2As_2O_5]_8(C_6H_5AsO_3)_2(C_6H_5AsO_3H)_2(H_2AsO_4)_4(H_2O)_3\} \cdot 2H_2O$ and $[H_3O]_6\{(UO_2)_{12}[(C_6H_5)_2As_2O_5]_{12}(C_6H_5AsO_3H)_6(H_2O)_5[H_2AsO_4(H_2O)_2][H_3O]\} \cdot H_2O$ [89] (Fig. 12a, b). In both structures the uranyl polyhedra are monomeric, and the first structure contains ten of these uranyl cations, eight of which are bound by eight pyroarsonate ligands. Two hydrogen arsenates and two phenylarsonates coordinate the remaining two polyhedra. Indeed, pyroarsonate is pliable and conducive with cage cluster formation. Similar to the carboxylate moieties in the uranyl-carboxyphosphonate clusters, the phenyl rings of the phenylarsonate groups project outwards on the periphery of the structures, while the arsonate unit is bound to the uranyl cations as part of the core cage structure.

The second structure, $[H_3O]_6\{(UO_2)_{12}[(C_6H_5)_2As_2O_5]_{12}(C_6H_5AsO_3H)_6(H_2O)_5[H_2AsO_4(H_2O)_2][H_3O]\} \cdot H_2O$, also has two distinct coordination environments for uranyl polyhedra: six uranyl cations bound by 12 pyroarsonate groups and two unique triangular units, where three uranyl cations are connected by three phenylarsonates. The cage encapsulates a hydrogen arsenate in octahedral coordination. These structures have only been observed crystallographically, and their assembly in solution prior to crystallization and persistence in solution subsequent to dissolution has not been demonstrated.

Two uranyl calixarene carboxylate cage structures were reported by Pasquale et al. [63] that contain 8 and 20 uranyl polyhedra (Fig. 13a). The calixarene carboxylates are located on the faces of the cages. The first cage is in the space group *Fm-3m* and contains 6 calixarene units and 8 uranyl hexagonal bipyramids. The second contains 12 calix[5]arene units and 20 uranyl ions. Also, octanuclear cages, dodecanuclear rings, and hexadecanuclear cages have been synthesized with Cu(II) or Ni(II) and Kemp's triacid (Fig. 13b) [90, 91].

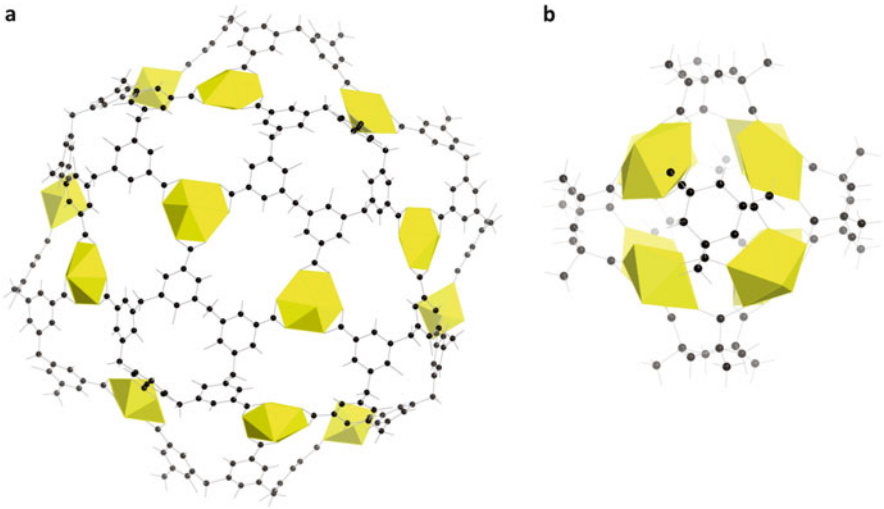

Fig. 13 (**a**) The dodecanuclear uranyl calixarene carboxylate cage cluster and (**b**) an octanuclear Kemp's triacid cluster

5 Hybrid Actinide and Transition Metal Clusters

The science of transition metal oxide clusters, commonly referred to as polyoxometalates (POMs), began long before the actinide clusters – the first POM, ammonium 12-molybdophosphate or $(NH_4)_3PMo_{12}O_{40}aq$, was described nearly 240 years ago, although it was not until much later that it was understood [92]. This field continues to advance centuries later, as an abundance of new structures with potentially useful properties are continuously discovered. Recently, actinyl peroxide cage clusters have emerged and have been compared to transition metal polyoxometalates in detail by Nyman and Burns [26]. Similarities between actinides and the d-block elements include the ability to attain multiple oxidation states and, perhaps most importantly, multiply bonding to terminal *–yl* O atoms. Like An(V) and An(VI), d^0 closed shell transition metals V(V), Nb(V), Ta(V), Mo (VI), and W(VI) may possess one or two *–yl* oxygen atoms. In contrast to actinyl O atoms, *–yl* oxygen atoms bound to transition metals are usually in a *cis* arrangement; therefore, *–yl* oxygen atoms terminate only one surface of a transition metal cluster.

The Keplerates are perhaps the most structurally similar transition metal POMs to the actinyl peroxide cage [93, 94]. These spherical POMs exist as two types: $\{M_{72}M'_{30}\}$ where M = Mo, M' = V(IV), Cr(III), Fe(III), Mo(V) and $\{M_{72}Mo_{60}\}$ where M = Mo, W [95]. Like Keplerate structures, uranyl peroxide cage clusters have similar properties such as stability in solution and the ability to exchange encapsulated cations [93]. Both have also been observed to further assemble into blackberry structures in solution [96, 97].

Nyman and Burns [26] expanded the comparison of actinyl clusters to transition metal POMs by including the broader acidic and alkaline groups of transition metals. Uranyl clusters display similarities with both groups, such as self-assembly in basic conditions and forming stable bonds with peroxide, like the alkaline transition metals. On the other hand, they also display alkali ion-associated solubility trends that are akin to the acidic transition metals. The authors also observed that Nb and Ta both form stable bonds with peroxide, but only Nb/Ta$(O_2)_4$ centered U clusters have been published. Commonalities such as these promote the idea that the two fields may meet and that hybrid structures may be realized [26].

The first transition metal polyoxometalate containing uranium was $[Na_2(UO_2)_2(PW_9O_{34})_2]^{12-}$, published by Kim et al. [98]. Other studies have reported structures of transition metal polyoxometalates that incorporate actinide cations as addenda atoms, such as sandwich complexes bridged by actinide cations. Examples include tri-lacunary heteropolyoxotungstates, which have been bridged by U, Np, and Pu cations [12, 99–104]. Previous reviews have described other hybrid actinyl-transition metal structures including a large transition metal and thorium cluster that has a core composition of $[Th_6Mn_{10}O_{22}(OH)_2]^{18+}$ [105]. Uranyl peroxide units were first incorporated into polyoxometalate structures with the synthesis of the U-shaped 36-tungsto-8-phoshate cluster containing two uranyl peroxide units, which has the total cluster composition $LiK_4\{(UO_2)_4(\mu\text{-}O_2)_4(H_2O)_2(PO_3OH)_2P_6W_{36}O_{136}\}^{25-}$ [106].

5.1 Wheel-Shaped Structures

The wheel-shaped uranyl peroxide tungstometalate $\{[W_5O_{21}]_3[UO_2)_2(\mu\text{-}O_2)]_3\}^{30-}$, published by Miro et al. [107], is an example of a hybrid transition metal-actinide POM (Fig. 14a). Very recently, a peroxide-free wheel-shaped cluster, $(EMIm)_{15}Na_5[(UO_2)_{20}(V_2O_7)_{10}\text{-}(SO_4)_{10}]\cdot 80H_2O$ (EMIm is 3-ethyl-1-methylimidazolium), was obtained using ionic liquids (Fig. 14b, c) [62]. U(VI) is in pentagonal bipyramidal geometry, and vanadium(V) is in square pyramidal coordination. The structure also includes 10 sulfate tetrahedra. Typical of POMs, vanadyl O atoms terminate the cluster, as do the uranyl O atoms. The wheel consists of two 10-membered rings of uranyl bipyramids linked by vertex-sharing to the two adjacent polyhedra. Five sulfate tetrahedra on the top and bottom of the wheel connect three uranyl polyhedra by vertex-sharing, giving the ten-membered rings rigidity. Edge-sharing dimers of vanadate polyhedra link the two uranyl sulfate rings by sharing two additional edges each with adjacent uranyl polyhedra. The dimers are also linked to each other by vertex-sharing. Na and 10 H_2O groups are encapsulated in the cluster and the exterior contains EMIm cations and disordered H_2O.

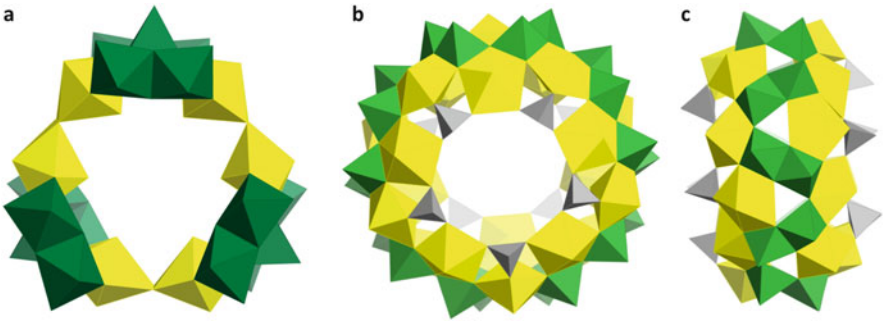

Fig. 14 Wheel-shaped hybrid transition metal clusters synthesized to date, including (**a**) $\{[W_5O_{21}]_3[U^{VI}O_2]_2(\mu\text{-}O_2)]_3\}^{30-}$ and (**b** and **c**) $U_{20}V_{20}$, with vanadium or tungsten polyhedra in *green*, and sulfate in *gray*

5.2 Hybrid Closed-Cage Structures

In the past few years, progress has been made toward transition metal incorporation into uranyl peroxide cages, where uranyl polyhedra and transition metal polyhedra are both essential components of the cage wall. Adelani et al. [108] used Ni to synthesize the first complete hybrid cage, $[H_3O]_4[Ni(H_2O)_3]_4\{Ni[(UO_2)\text{-}(PO_3C_6H_4CO_2)]_3(PO_4H)\}_4 \cdot 2.72H_2O$, although its presence in solution was not demonstrated. In contrast to the hexagonal bipyramids in most uranyl peroxide cage clusters, this cluster has only pentagonal bipyramids that share edges to form dimers (Fig. 15). It contains six dimers of uranyl pentagonal bipyramids in addition to eight Ni(II) octahedra, four of which are included in the core structure by sharing three vertices with uranyl bipyramids and phosphonate groups. The remaining Ni (II) polyhedra are located on the exterior of the cluster, where they are held onto the structure by the 2-carboxyphenyl phosphonate ligands. The phenyl groups of the 2-carboxyphenylphosphonate ligands extend from the core structure and are the terminal ligands.

More recently, Ling et al. [76] reported several hybrid uranyl-transition metal cage clusters ($U_{50}W_6P_{20}$, $U_{44}Mo_2P_{16}$, $U_{28}W_4P_{12}$, $U_{28}Mo_4P_{12}$,$U_{18}W_2P_{12}$, and $U_{48}W_6P_{48}$) containing uranyl peroxide polyhedra, tungsten or molybdenum units, and phosphate tetrahedra. Compared to previously described cage clusters, these six clusters have novel topologies and configurations of U(VI), including rings of polyhedra containing 7, 8, 10, and 12 members. These rings are the largest in uranyl peroxide cage clusters that do not form equatorial belts around their clusters, a configuration that is possible because select peroxo ligands are in a *trans* arrangement. This was only previously reported for belts of uranyl polyhedra in $U_{22}PO_3$ and $U_{28}PO_3$ [60]. Tungsten and molybdenum may play the role of stabilizing rings of polyhedra, where they share vertices with uranyl polyhedra. All of these structures contain Li counterions that, although not resolved in the crystal

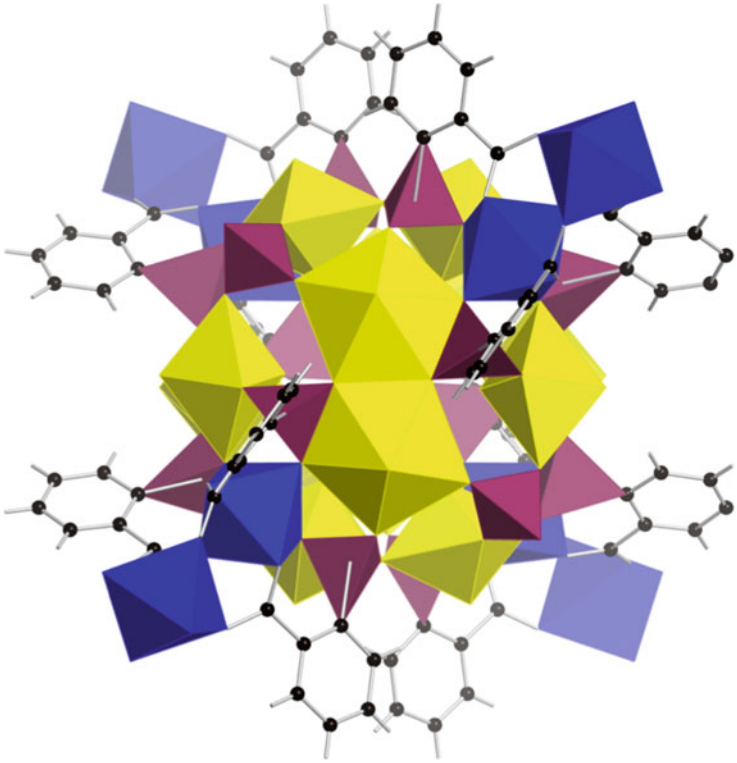

Fig. 15 The hybrid closed-cage structure $[H_3O]_4[Ni(H_2O)_3]_4\{Ni[(UO_2)\text{-}(PO_3C_6H_4CO_2)]_3(PO_4H)\}_4 \cdot 2.72H_2O$. Ni(II) polyhedra are *blue* and phosphonate groups are in *pink*

structures, are presumed to be encapsulated by and located on the outside of the clusters to balance negative charges.

$U_{50}W_6P_{20}$ and $U_{44}Mo_2P_{16}$ [76] contain uranyl in hexagonal bipyramidal coordination (Fig. 16a, b). The majority of the hexagonal bipyramids are analogous to those found in most uranyl peroxide cage clusters: three edges are shared with adjacent polyhedra and two of the shared edges are peroxide bridges in a *cis* configuration. $U_{44}Mo_2P_{16}$ also has hexagonal bipyramids with only one bidentate peroxide group. $U_{50}W_6P_{20}$ and $U_{44}Mo_2P_{16}$ have an additional 18 and 14 uranyl hexagonal bipyramids, respectively, that share edges with only two other polyhedra through peroxide bridges in *trans* configuration. Two of these polyhedra in $U_{44}Mo_2P_{16}$ are unique because they also share vertices with each other, resulting in tetramers formed by vertex- and edge-sharing. Both clusters have six-membered rings of edge-sharing polyhedra that are analogous to those described previously for uranyl peroxide cage clusters, and $U_{44}Mo_2P_{16}$ also has five-membered rings of polyhedra.

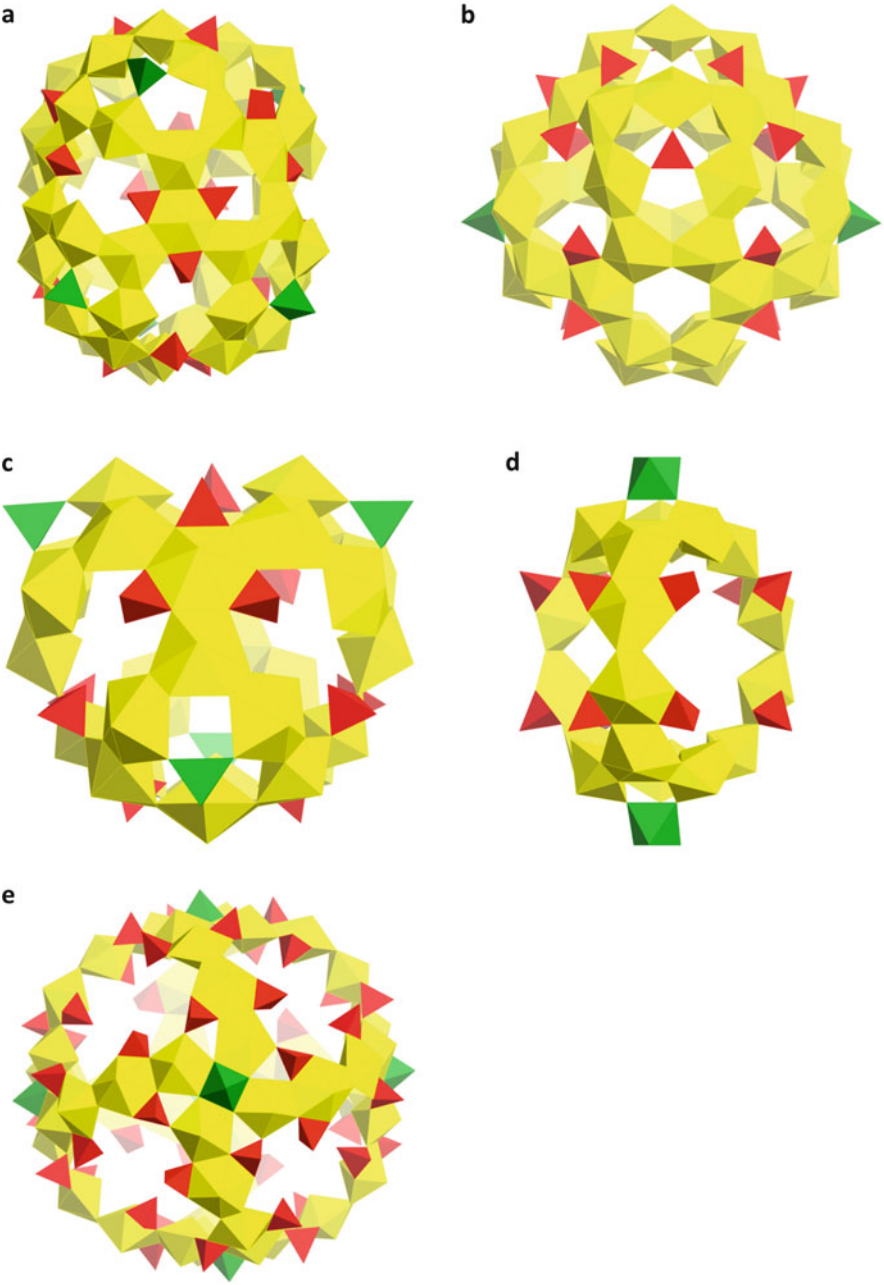

Fig. 16 (**a**) $U_{50}W_6P_{20}$, (**b**) $U_{44}Mo_2P_{16}$, (**c**) $U_{28}W_4P_{12}$, (**c**) $U_{28}Mo_4P_{12}$, (**d**) $U_{18}W_2P_{12}$, and (**e**) $U_{48}W_6P_{48}$ are shown. W and Mo tetrahedra are both *green* and phosphate are *red*

The *trans* configuration of peroxide groups about uranyl allows the formation of novel seven- and eight-membered rings of uranyl polyhedra in both $U_{50}W_6P_{20}$ and $U_{44}Mo_2P_{16}$. Each of the eight-membered rings features two $(H_2PO_4)^-$ tetrahedra that are bidentate to the uranyl polyhedra and extend into the voids of the rings. The voids of the seven-membered rings contain the transition metal polyhedra, $(WO_3OH)^-$ and $(MoO_3OH)^-$ for $U_{50}W_6P_{20}$ and $U_{44}Mo_2P_{16}$, respectively. The tetrahedra share vertices with three uranyl polyhedra of the ring, dividing the seven-membered rings into two topological squares and a pentagon. $U_{44}Mo_2P_{16}$ has four seven-membered rings but only two $(MoO_3OH)^-$ tetrahedra – the two remaining seven-membered rings have $(HPO_4)^{2-}$ tetrahedra located at the center.

$U_{28}W_4P_{12}$ and $U_{28}Mo_4P_{12}$ [76] are isostructural clusters that contain $(WO_3OH)^-$ or $(MoO_3OH)^-$ tetrahedra, respectively (Fig. 16c). *Trans* U-O_2-O bridges in the structure yield eight-membered rings analogous to those in $U_{50}W_6P_{20}$ and $U_{44}Mo_2P_{16}$, with two bidentate $(H_2PO_4)^-$ tetrahedra that extend into the void of the ring. In contrast to the previously described clusters, $(WO_3OH)^-$ or $(MoO_3OH)^-$ tetrahedra are coordinated to uranyl ions at the center of six-membered rings instead of seven-membered rings. These six-membered rings contain alternating two-edge-sharing polyhedra, with peroxide in *trans* configuration, and three-edge-sharing polyhedra.

A more definitive departure from typical uranyl peroxide cage cluster topologies is displayed by the cluster $U_{18}W_2P_{12}$, which has two $(WO_3(OH)_3)^{3-}$ octahedra and 12 $(H_2PO_4)^-$ tetrahedra in addition to uranyl hexagonal bipyramids (Fig. 16d). The majority of uranyl polyhedra make up three 10-membered rings of polyhedra that extend from pole to pole, unlike any previously reported configuration for uranyl peroxide cage clusters. The polar regions are terminated by two six-membered rings of uranyl polyhedra that are topologically identical to those in $U_{28}W_4P_{12}$ and $U_{28}Mo_4P_{12}$; however, $(WO_3(OH)_3)^{3-}$ octahedra share three vertices with uranyl polyhedra, dividing the ring into three topological squares. $U_{18}W_2P_{12}$is the first example of a uranyl peroxide cage cluster that has direct linkages between clusters. $(WO_3(OH)_3)^{3-}$ octahedra share faces with $(WO_3(OH)_3)^{3-}$ octahedra of the neighboring cluster, connecting the $U_{18}W_2P_{12}$ clusters into chains.

The remaining hybrid uranyl-transition metal peroxide cage cluster synthesized by Ling et al. [76] is $U_{48}W_6P_{48}$, which has 6 $(WO_4OH)^{3-}$ square pyramids, 24 $(HPO_4)^{2-}$ tetrahedra, and 24 $(H_2PO_4)^-$ tetrahedra (Fig. 16e). The uranyl configuration of this cluster is similar to $U_{22}PO_3$ [60] in that it contains U-O_2-U bridged hexagonal bipyramids that share exclusively two edges and that are incorporated into four-membered belts terminated by pentagonal bipyramids. Unlike $U_{22}PO_3$, where peroxide bridges the hexagonal and pentagonal bipyramids, the hexagonal bipyramids in $U_{48}W_6P_{48}$ share edges with pentagonal bipyramids through O atoms donated by bidentate $(H_2PO_4)^-$ tetrahedra. The uranyl pentagonal bipyramids also share two vertices with adjacent pentagonal bipyramids. This cluster is the first cage cluster to have 12-membered rings of uranyl polyhedra although it has a relatively simple topology composed of only 4- and 12-membered rings. The six tetramers are made up of four vertex-sharing pentagonal bipyramids coordinated at the center by

the $(WO_4OH)^{3-}$ square pyramids. Each of the polyhedra in the four-membered ring is shared with the two of the four adjacent 12-membered rings.

6 Conclusions

Despite being a relatively new field of study, there is already an extensive library of actinide oxo clusters, especially in the case of uranyl peroxide cage clusters. It is now apparent that the topological and compositional complexity of actinide oxo clusters rivals that found for transition metal polyoxometalates over the past several decades. Many more variations in actinide oxo clusters will likely be described over the next few years. Efforts focused on potential applications in the nuclear-fuel cycle may also be fruitful, as the behavior of actinide oxo clusters in solution will in many cases be markedly different from that of simple species. Conditions in nuclear accident scenarios, such as where water is interacting with the damaged reactor cores at Fukushima, Japan, and in geologic repositories for nuclear waste, are potentially conducive to formation of actinide oxo clusters, in which case they may be important for environmental transport of actinides and repository performance.

Acknowledgements This research is funded by the Office of Basic Energy Sciences of the US Department of Energy as part of the Materials Science of Actinides Energy Frontiers Research Center (DE-SC0001089).

References

1. Neidig ML, Clark DL, Martin RL (2013) Covalency in f-element complexes. Coord Chem Rev 257(2):394–406
2. Morss LR et al (2006) In: Morss LR, Edelstein NM, Fuger J, Katz JJ (ed) The chemistry of the actinide and transactinide elements, 3rd edn. Springer, Dordrecht
3. Cary SK et al (2015) Emergence of californium as the second transitional element in the actinide series. Nat Commun 6:8
4. Maly J et al (1968) Nobelium - tracer chemistry of divalent and trivalent ions. Science 160 (3832):1114
5. Polinski MJ et al (2014) Unusual structure, bonding and properties in a californium borate. Nat Chem 6(5):387–392
6. Abdelouas A (2006) Uranium mill tailings: geochemistry, mineralogy, and environmental impact. Elements 2(6):335–341
7. Kersting AB et al (1999) Migration of plutonium in ground water at the Nevada Test Site. Nature 397(6714):56–59
8. Stubbs JE et al (2009) Newly recognized hosts for uranium in the Hanford Site vadose zone. Geochimica Et Cosmochimica Acta 73(6):1563–1576
9. Knope KE et al (2012) Thorium(IV)-selenate clusters containing an octanuclear Th (IV) hydroxide/oxide core. Inorg Chem 51(7):4239–4249

10. Wylie EM et al (2014) Ultrafiltration of URANYL PEROXIDE NANOCLUSTERS FOR THE SEPARATION OF URANIUM FROM AQUEOUS SOLUTION. ACS Appl Mater Interfaces 6(1):473–479
11. Qiu J, Burns PC (2013) Clusters of actinides with oxide, peroxide, or hydroxide bridges. Chem Rev 113(2):1097–1120
12. Copping R et al (2009) Probing the 5f electrons in a plutonyl(VI) cluster complex. Dalton Trans 29:5609–5611
13. Denning RG et al (2002) Covalency in the uranyl ion: a polarized x-ray spectroscopic study. J Chem Phys 117(17):8008–8020
14. Denning RG (2007) Electronic structure and bonding in actinyl ions and their analogs. J Phys Chem A 111(20):4125–4143
15. Burns PC, Ewing RC, Hawthorne FC (1997) The crystal chemistry of hexavalent uranium: polyhedron geometries, bond-valence parameters, and polymerization of polyhedra. Can Mineral 35:1551–1570
16. Denning RG (1992) Electronic-structure and bonding in actinyl ions. Struct Bond 79:215–276
17. La Pierre HS et al (2015) Charge control of the inverse trans-influence. Chem Commun 51 (93):16671–16674
18. La Pierre HS, Meyer K (2013) Uranium-ligand multiple bonding in uranyl analogues, L=U=L (n+), and the inverse trans influence. Inorg Chem 52(2):529–539
19. O'Grady E, Kaltsoyannis N (2002) On the inverse trans influence. Density functional studies of MOX(5) (n-) (M=Pa, n=2; M=U, n=1; M=Np, n=0; X=F, Cl or Br). J Chem Soc Dalton Trans 2002(6):1233–1239
20. Chermette H, Rachedi K, Volatron F (2006) Trans effect and inverse trans effect in MLX5 complexes (M=Mo, U; L=O, S; X=Cl, Br): a rationalization within density functional theory study. J Mol Struct THEOCHEM 762(1–3):109–121
21. Burns PC (2005) U6+ minerals and inorganic compounds: insights into an expanded structural hierarchy of crystal structures. Can Mineral 43:1839–1894
22. Forbes TZ, Wallace C, Burns PC (2008) Neptunyl compounds: polyhedron geometries, bond-valence parameters, and structural hierarchy. Can Mineral 46:1623–1645
23. Krot NN, Grigoriev MS (2004) Cation-cation interaction in crystalline actinide compounds. Uspekhi Khimii 73(1):94–106
24. Duval PB et al (2001) Synthesis and structural characterization of the first uranium cluster containing an isopolyoxometalate core. Angew Chem Int Ed 40(18):3358
25. Burns PC et al (2005) Actinyl peroxide nanospheres. Angew Chem Int Ed 44(14):2135–2139
26. Nyman M, Burns PC (2012) A comprehensive comparison of transition-metal and actinyl polyoxometalates. Chem Soc Rev 41(22):7354–7367
27. Salmon L, Thuery P, Ephritikhine M (2006) Polynuclear uranium(IV) compounds with (mu (3)-oxo)U-3 or (mu(4)-oxo)U-4 cores and compartmental Schiff base ligands. Polyhedron 25 (7):1537–1542
28. Rogers RD, Bond AH, Witt MM (1991) Macrocycle complexation chemistry 34. Polyethylene-glycol and glycolate complexes of Th^{4+}. Preparation and structural characterization of $ThCl_3$(Pentaethylene glycol) $Cl.CH_3CN$ and the $(Th^{4+})_4$ cluster, $[Th_4Cl_8(O)$ (Tetraethylene glycolate)$_3$].$3CH_3CN$. Inorg Chim Acta 182(1):9–17
29. Brianese N et al (1989) Reactivity of dicyclopentadienyluranium(IV) derivatives: formation and structural characterization of an oxygen bridged cluster containing both inorganic and organometallic uranium atoms. J Organomet Chem 365(3):223–232
30. Diwu J, Wang S, Albrecht-Schmitt TE (2012) Periodic trends in hexanuclear actinide clusters. Inorg Chem 51(7):4088–4093
31. Hennig C et al (2012) Structure and stability range of a hexanuclear Th(IV)-glycine complex. Dalton Trans 41(41):12818–12823
32. Hu YJ et al (2013) Understanding the ligand-directed assembly of a hexanuclear Th-IV molecular cluster in aqueous solution. Eur J Inorg Chem 2013(24):4159–4163

33. Knope KE et al (2011) Thorium(IV) molecular clusters with a hexanuclear Th core. Inorg Chem 50(19):9696–9704
34. Takao K et al (2012) Formation of soluble hexanuclear neptunium(IV) Nanoclusters in aqueous solution: growth termination of actinide(IV) hydrous oxides by carboxylates. Inorg Chem 51(3):1336–1344
35. Takao S et al (2009) First hexanuclear UIV and ThIV formate complexes – structure and stability range in aqueous solution. Eur J Inorg Chem 2009(32):4771–4775
36. Vasiliu M et al (2012) Spectroscopic and energetic properties of thorium(IV) molecular clusters with a hexanuclear core. J Phys Chem A 116(25):6917–6926
37. Zhang Y et al (2015) Synthesis, spectroscopic characterization and crystal structures of thorium(IV) mononuclear lactato and hexanuclear formato complexes. Polyhedron 87:377–382
38. Berthet J-C, Thuery P, Ephritikhine M (2010) Formation of uranium(IV) oxide clusters from uranocene U(eta(8)-C8H8)(2) and uranyl UO2X2 compounds. Inorg Chem 49 (17):8173–8177
39. Nocton G et al (2010) Ligand assisted cleavage of uranium oxo-clusters. Chem Commun 46 (16):2757–2759
40. Knope KE, Soderholm L (2013) Plutonium(IV) cluster with a hexanuclear Pu-6(OH)(4)O-4 (12+) core. Inorg Chem 52(12):6770–6772
41. Pan L et al (2008) Synthesis and structural determination of a hexanuclear zirconium glycine compound formed in aqueous solution. Inorg Chem 47(13):5537–5539
42. Lundgren G (1956) The crystal structure of Ce6O4(OH)4(SO4)6. Ark Kemi 10(2):183–197
43. Miersch L et al (2010) A novel water-soluble hexanuclear bismuth oxido cluster - synthesis, structure and complexation with polyacrylate. Eur J Inorg Chem 30:4763–4769
44. Diwu J et al (2011) Self-assembly of hexanuclear clusters of 4f and 5f elements with cation specificity. Eur J Inorg Chem 2011(9):1374–1377
45. Falaise C et al (2013) Three-dimensional MOF-type architectures with tetravalent uranium hexanuclear motifs (U6O8). Chemistry 19(17):5324–5331
46. Xiao B et al (2015) Chemical and structural evolution in the Th-SeO32-/SeO42- system: from simple selenites to cluster-based selenate compounds. Inorg Chem 54(6):3022–3030
47. Biswas B et al (2011) Base-driven assembly of large uranium oxo/hydroxo clusters. Angew Chem Int Ed 50(25):5744–5747
48. Woidy P, Kraus F (2014) Th-10(mu-F-16)(mu(3)-O-4)(mu(4)-O-4)(NH3)(32) (NO3)(8) center dot 19.6 NH3 - the largest thorium complex from solution known to date. Zeitschrift Fur Anorganische Und Allgemeine Chemie 640(8–9):1547–1550
49. Nocton G et al (2007) Self-assembly of polyoxo clusters and extended frameworks by controlled hydrolysis of low-valent uranium. Angew Chem Int Ed 46(40):7574–7578
50. Soderholm L et al (2008) The structure of the plutonium oxide nanocluster Pu38O56Cl54 (H2O)(8) (14-). Angew Chem Int Ed 47(2):298–302
51. Wilson RE, Skanthakumar S, Soderholm L (2011) Separation of plutonium oxide nanoparticles and colloids. Angew Chem Int Ed 50(47):11234–11237
52. Powell BA et al (2004) Pu(V)O-2(+) adsorption and reduction by synthetic magnetite (Fe3O4). Environ Sci Technol 38(22):6016–6024
53. Powell BA et al (2005) PU(V)0(2)(+) adsorption and reduction by synthetic hematite and goethite. Environ Sci Technol 39(7):2107–2114
54. Zimmerman T, Zavarin M, Powell BA (2014) Influence of humic acid on plutonium sorption to gibbsite: determination of Pu-humic acid complexation constants and ternary sorption studies. Radiochim Acta 102(7):629–643
55. Hixon AE, Powell BA (2014) Observed changes in the mechanism and rates of Pu (V) reduction on hematite as a function of total plutonium concentration. Environ Sci Technol 48(16):9255–9262
56. Powell BA et al (2011) Stabilization of plutonium nano-colloids by epitaxial distortion on mineral surfaces. Environ Sci Technol 45(7):2698–2703

57. Falaise C et al (2013) Isolation of the large {Actinide}(38) poly-oxo cluster with uranium. J Am Chem Soc 135(42):15678–15681
58. Copping R et al (2012) A tetrameric neptunyl(v) cluster supported by a Schiff base ligand. Dalton Trans 41(36):10900–10902
59. Mougel V et al (2009) Stable pentavalent uranyl species and selective assembly of a polymetallic mixed-valent uranyl complex by cation-cation interactions. Angew Chem Int Ed 48(45):8477–8480
60. Qiu J et al (2013) Time-resolved assembly of chiral uranyl peroxo cage clusters containing belts of polyhedra. Inorg Chem 52(1):337–345
61. Burns PC (2011) Nanoscale uranium-based cage clusters inspired by uranium mineralogy. Mineral Mag 75(1):1–25
62. Senchyk GA et al (2015) Hybrid uranyl-vanadium nano-wheels. Chem Commun 51 (50):10134–10137
63. Pasquale S et al (2012) Giant regular polyhedra from calixarene carboxylates and uranyl. Nat Commun 3:785
64. Sigmon GE et al (2009) Symmetry versus minimal pentagonal adjacencies in uranium-based polyoxometalate fullerene topologies. Angew Chem Int Ed 48(15):2737–2740
65. Kroto HW et al (1985) C-60 - buckminsterfullerene. Nature 318(6042):162–163
66. Sigmon GE et al (2009) Crown and bowl-shaped clusters of uranyl polyhedra. Inorg Chem 48 (23):10907–10909
67. Ling J, Qiu J, Burns PC (2012) Uranyl peroxide oxalate cage and core-shell clusters containing 50 and 120 uranyl ions. Inorg Chem 51(4):2403–2408
68. Qiu J et al (2012) Time-resolved self-assembly of a fullerene-topology core-shell cluster containing 68 uranyl polyhedra. J Am Chem Soc 134(3):1810–1816
69. Qiu J et al (2014) Water-soluble multi-cage super tetrahedral uranyl peroxide phosphate clusters. Chem Sci 5(1):303–310
70. Ling J et al (2010) Uranium pyrophosphate/methylenediphosphonate polyoxometalate cage clusters. J Am Chem Soc 132(38):13395–13402
71. Forbes TZ et al (2008) Metal-oxygen isopolyhedra assembled into fullerene topologies. Angew Chem Int Ed 47(15):2824–2827
72. Burns PC, Ewing RC, Navrotsky A (2012) Nuclear fuel in a reactor accident. Science 335 (6073):1184–1188
73. Liu Y et al (2015) Extraction of uranyl peroxo clusters from aqueous solution by mesoporous silica SBA-15. J Radioanal Nucl Chem 303(3):2257–2262
74. Unruh DK et al (2011) Complex nanoscale cage clusters built from uranyl polyhedra and phosphate tetrahedra. Inorg Chem 50:5509–5516
75. Sigmon GE et al (2009) Uranyl-peroxide interactions favor nanocluster self-assembly. J Am Chem Soc 131(46):16648
76. Ling J et al (2014) Hybrid uranium-transition-metal oxide cage clusters. Inorg Chem 53 (24):12877–12884
77. Vlaisavljevich B, Gagliardi L, Burns PC (2010) Understanding the structure and formation of uranyl peroxide nanoclusters by quantum chemical calculations. J Am Chem Soc 132 (41):14503–14508
78. Miro P et al (2010) On the origin of the cation templated self-assembly of uranyl-peroxide nanoclusters. J Am Chem Soc 132(50):17787–17794
79. Qiu J et al (2015) Cation templating and electronic structure effects in uranyl cage clusters probed by the isolation of peroxide-bridged uranyl dimers. Inorg Chem 54(9):4445–4455
80. Alam TM et al (2014) Solid-state dynamics of uranyl polyoxometalates. Chemistry 20 (27):8302–8307
81. Liao ZL, Deb T, Nyman M (2014) Elucidating self-assembly mechanisms of uranyl peroxide capsules from monomers. Inorg Chem 53(19):10506–10513
82. Nyman M, Rodriguez MA, Alam TM (2011) The U-28 nanosphere: what's inside? Eur J Inorg Chem 14:2197–2205

83. Ling J et al (2012) Uranyl peroxide pyrophosphate cage clusters with oxalate and nitrate bridges. Dalton Trans 41(24):7278–7284
84. Ling J et al (2010) Hybrid uranium-oxalate fullerene topology cage clusters. Angew Chem Int Ed 49(40):7271–7273
85. Adelani PO et al (2013) Hybrid uranyl-carboxyphosphonate cage clusters. Inorg Chem 52 (13):7673–7679
86. Liao ZL et al (2013) Cage clusters built from uranyl ions bridged through peroxo and 1-hydroxyethane-1,1-diphosphonic acid ligands. Dalton Trans 42(19):6793–6802
87. Burns PC, Hughes KA (2003) Studtite, (UO2)(O-2)(H2O)(2) (H2O)(2): the first structure of a peroxide mineral. Am Mineral 88(7):1165–1168
88. Qiu J et al (2014) Expanding the crystal chemistry of uranyl peroxides: four hybrid uranyl-peroxide structures containing EDTA. Inorg Chem 53(22):12084–12091
89. Adelani PO, Sigmon GE, Burns PC (2013) Hybrid uranyl arsonate coordination nanocages. Inorg Chem 52(11):6245–6247
90. Thuery P (2014) Increasing complexity in the Uranyl Ion-Kemp's Triacid System: from one- and two-dimensional polymers to uranyl-copper(II) dodeca- and hexadecanuclear species. Cryst Growth Des 14(5):2665–2676
91. Thuery P (2014) A highly adjustable coordination system: nanotubular and molecular cage species in uranyl ion complexes with Kemp's triacid. Cryst Growth Des 14(3):901–904
92. Berzelius JJ (1826) Poggend. Ann Phys Chem 6:369
93. Muller A et al (1998) Organizational forms of matter: an inorganic super fullerene and Keplerate based on molybdenum oxide. Angew Chem Int Ed 37(24):3360–3363
94. Kortz U et al (2009) Polyoxometalates: fascinating structures, unique magnetic properties. Coord Chem Rev 253(19–20):2315–2327
95. Muller A, Gouzerh P (2012) From linking of metal-oxide building blocks in a dynamic library to giant clusters with unique properties and towards adaptive chemistry. Chem Soc Rev 41(22):7431–7463
96. Liu TB (2002) Supramolecular structures of polyoxomolybdate-based giant molecules in aqueous solution. J Am Chem Soc 124(37):10942–10943
97. Li D et al (2014) Evolution of actinyl peroxide clusters U-28 in dilute electrolyte solution: exploring the transition from simple ions to macroionic assemblies. Chemistry 20 (6):1683–1690
98. Kim K-C, Pope MT (1999) Cation-directed structure changes in polyoxometalate chemistry. Equilibria between isomers of Bis(9-tungstophosphatodioxouranate(VI)) complexes. J Am Chem Soc 121(37):8512–8517
99. Berg JM et al (2015) Unexpected actinyl cation-directed structural variation in neptunyl (VI) A-type tri-lacunary heteropolyoxotungstate complexes. Inorg Chem 54(9):4192–4199
100. Kim KC, Gaunt A, Pope MT (2002) New heteropolytungstates incorporating dioxouranium (VI). Derivatives of alpha- SiW9O34 (10-), alpha- AsW9O33 (9-), gamma- SiW10O36 (8-), and As4W40O140 (28-). J Clust Sci 13(3):423–436
101. Khoshnavazi R et al (2007) Syntheses and structural determination of new bis (9-tungstoarsenato)tris(dioxouranate(VI)) and its mono oxovanadate(IV) derivative complexes. Inorg Chim Acta 360(2):686–690
102. Tan RX et al (2006) Polyoxotungstates containing uranyl group: Germanotungstates with Keggin sandwich structure. Inorg Chem Commun 9(12):1331–1334
103. Khoshnavazi R et al (2006) Syntheses and structures determination of new polytungstoarsenates Na2As2W18U2O72 (12-) and MAs2W18U2O72 (13-) (M=NH4+ and K+). Polyhedron 25(9):1921–1926
104. Gaunt AJ et al (2002) The first structural and spectroscopic characterization of a neptunyl polyoxometalate complex. J Am Chem Soc 124(45):13350–13351
105. Mishra A et al (2007) High-nuclearity Ce/Mn and Th/Mn cluster chemistry: preparation of complexes with Ce4Mn10O10(OMe)(6) (18+) and Th6Mn10O22(OH)(2) (18+) cores. Inorg Chem 46(8):3105–3115

106. Mal SS, Dickman MH, Kortz U (2008) Actinide polyoxometalates: incorporation of uranyl-peroxo in U-shaped 36-tungsto-8-phosphate. Chemistry 14(32):9851–9855
107. Miro P et al (2012) Experimental and computational study of a new wheel-shaped {W5O21 (3) ((UO2)-O-VI)(2)(mu-O-2) (3)}(30-) polyoxometalate. Inorg Chem 51(16):8784–8790
108. Adelani PO, Oliver AG, Albrecht-Schmitt TE (2012) Uranyl heteropolyoxometalate: synthesis, structure, and spectroscopic properties. Inorg Chem 51(9):4885–4887